2

Modelling of DC-to-DC Power Converters

2.1 Introduction

In this chapter, we derive the dynamic models of DC-to-DC power converters. The most elementary structures of these converters are broadly classified into *second order converters* and *fourth order converters*. In attention to the number of independent switches they are classed into two groups: *mono-variable*, or *Single Input Single Output* (SISO), and *multi-variable*, or *Multiple Input Multiple Outputs* (MIMO). The most commonly used converters correspond to the SISO second order converters. The advantages and difficulties of the MIMO converters is just beginning to be fully understood. We remark that there are converters with *multiple dependent* switches. These may still be SISO or MIMO. The second order converters that we study in this book are: the Buck converter, the Boost converter, the Buck-Boost converter and the non-inverting Buck-Boost converter. The fourth order converters are: the Cúk converter, the Sepic converter, the Zeta converter and the quadratic Buck converter. Some multi-variable converters can be obtained by a simple cascade arrangement of the basic SISO converter topologies while considering the switch in each stage as being completely independent of the other switches present in the arrangement. Many books in the Power Electronics literature present derivations of the power converters models. For a rather thorough presentation of the Euler-Lagrange modelling technique in DC-to-DC power converters, the reader is referred to the book by Ortega *et al.* [48]. The authors find the pioneering book by Severns and Bloom [54] quite accessible and direct. The thoughtful book by Kassakian *et al.* [35] contains also detailed derivations of the most popular DC-to-DC power converters topologies. Standard reference textbooks, which do contain models of DC-to-DC power converters but with a special emphasis on the steady state PWM switched behavior, are those of Bose [4], Czaki *et al.* [8], Rashid [50], Mohan *et al.* [44], Wood [79] and Batarseh [1].

We extensively use, in the derivation of the dynamic controlled models of the several converters, the fundamental Kirchoff's current and Kirchoff's voltage laws. The methodology for the derivation of the models is, therefore, quite straightforward. We fix the position of the switch, or switches, and derive the differential equations of the circuit model. We then combine the derived models into a single one parameterized by the switch position function whose value must coincide, for each possible case, with the numerical values of either "zero" or "one". In other words, the numerical values ascribed to the switch position function is the binary set $\{0, 1\}$. The obtained switched model is then interpreted as an *average model* by letting the switch position function take values on the closed interval of the real line $[0, 1]$. This state averaging procedure has been extensively justified in the literature since the early days of power electronics and, therefore, we do not dwell into the theoretical justifications of such averaging procedure. The consequences of this idealization will not be counterproductive in the controller design procedure, nor in its actual implementation through Pulse Width Modulated (PWM) "electronic actuators" or its corresponding sliding mode counterparts. In order to simplify the exposition, we make no distinction between the average model variables and the switched model variables. At the beginning, we shall only distinguish between these models by using u_{av} for the control input variable in the average model and by using u for the switched model. In later chapters, we shall also lift this distinction. It will be clear from the context whether we are referring to the average or to the switched model.

After the derivation of the average model of each converter, we systematically proceed to *normalize* the controlled differential equations constituting the dynamic model of each one of the studied converters. This normalization procedure has a definite advantage in the simulation of the converters and their derived controllers, aside from producing a rather simplified model of the system with as few parameters as possible. We point out that DC-to-DC power converters are somewhat difficult to simulate in computer packages, such as Simnon®, or MATLAB®, when considered in their traditional physical circuit form equations. This is due to the small values of inductances and capacitances which multiply the left hand sides of the involved differential equations. This fact produces quite large right hand sides thus making the model numerically "stiff" for computer simulations. The required numerical precision may then be achieved only at the cost of extremely small integration steps thus requiring longer simulation periods with a definite negative consequence in the trust placed on the obtained numerical precision. We, thus, evade these difficulties by resorting to normalization. We clarify that the normalization procedure not only refers to an appropriate scaling of the magnitudes of currents and voltages, but also to a re-scaling of the time variable to dimensionless units thus considerably simplifying the right hand side of the associated differential equations with an effective "acceleration" of the simulation time. This advantageous stand is achieved without sacrificing the required numerical precision. It is also quite straightforward to revert the normalization procedure, back to original variables magnitudes and time magnitudes, with a simple multiplication operation on the trajectories and time spans obtained for the normalized variables. Naturally, as long as actual laboratory implementation goes, the normalization considerably simplifies the controller design but the obtain design cannot be directly implemented. The actual gain values and expressions in the derived controllers have to be naturally "de-normalized" (i.e., placed in original physical units) before the implementation. We believe such an extra effort is worth the pain.

In the exposition about each converter, average models are utilized in establishing the average values of the equilibrium points. We usually parameterize the derived equilibrium points in terms of the desired average normalized value of the output voltage. Other parameterizations are still possible and, in fact, the normalized model equations allow us to carry them out with relative ease. The nature of the parametrization of the equilibrium points usually determines the fundamental characteristic of the converter in the sense that its static features define the amplifying, attenuating, or even both, features present in a specific converter. We refer to the static average normalized input-output relation as the *static transfer function.* This quantity is readily obtained from the average input value parametrization of the desired equilibrium output voltage.

2.2 The Buck Converter

The circuit diagram of the Buck converter is shown in Figure 2.1. In this figure, we actually depict the circuit schematic with the transistor-diode symbols. These arrangements constitute the actual synthesis, or realization, of the *switching* element. In Figure 2.2 however we show the ideal switch representation of the same converter circuit. In any of the two cases, the presented topological arrangement is addressed as the Buck converter. The Buck converter belongs to the class of "chopper" circuits, or attenuation circuits. It actually multiplies the constant input voltage E by a scalar factor, smaller than unity, at the output.

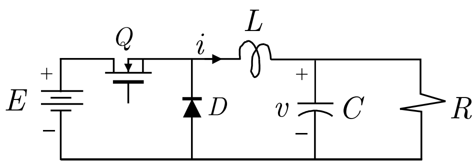

Fig. 2.1. Semiconductor realization of the Buck converter.

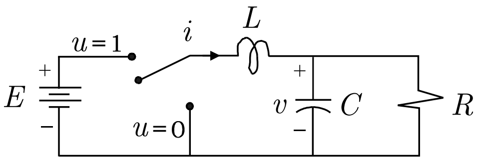

Fig. 2.2. Ideal switch representation of the Buck converter.

2.2.1 Model of the Converter

To obtain the differential equations describing the Buck converter, we consider the ideal topology shown in Figure 2.2. The system of differential equations describing the dynamics of the Buck converter is obtained through the direct application of Kirchoff's current and Kirchoff's voltage laws for each one of the possible circuit topologies arising from the assumed particular switch position function value. Thus, when the switch position function exhibits the value $u = 1$, we obtain the topology corresponding to the *non-conducting mode* for the diode. Alternatively, when the switch position exhibits the value $u = 0$ we obtain the second possible circuit topology corresponding to the *conducting mode* for the diode.

We first let the switch position function to be $u = 1$, and proceed to apply Kirchoff's current and Kirchoff's voltages laws to the resulting circuit (see Figure 2.3(a)). We obtain then the following system of differential equations:

$$\begin{aligned} L\frac{di}{dt} &= -v + E \\ C\frac{dv}{dt} &= i - \frac{v}{R} \end{aligned} \tag{2.1}$$

When the diode is in the non-conducting mode, i.e., when the switch position function is: $u = 0$ (see Figure 2.3(b)), the dynamics of the system is described by the following differential equations:

$$\begin{aligned} L\frac{di}{dt} &= -v \\ C\frac{dv}{dt} &= i - \frac{v}{R} \end{aligned} \tag{2.2}$$

By comparing the obtained particular dynamic systems descriptions, we immediately obtain the following *unified* dynamic system model. This results in:

$$\begin{aligned} L\frac{di}{dt} &= -v + uE \\ C\frac{dv}{dt} &= i - \frac{v}{R} \end{aligned} \tag{2.3}$$

Indeed, when $u = 1$ or $u = 0$, the model (2.3) recovers the system models (2.1) and (2.2), respectively. The Buck converter model is then represented by Equation 2.3. We usually refer to this model as the *switched model*, and, sometimes, we make emphasis on the binary valued nature of the switch position function u by using the set theoretic relation $u \in \{0, 1\}$.

The *average* converter model would be represented exactly by the same mathematical model (2.3), possibly by renaming the state variables with different symbols and by redefining the control variable u as a sufficiently smooth function taking values in the compact interval of the real line $[0, 1]$. In order to simplify the exposition, we shall refer to the model (2.3), with u replaced by u_{av}, as the *average model* and use it to derive average feedback control laws, for the average (continuous) input variable u_{av}. We shall however distinguish between the *average control input*, denoted by u_{av} and the *switched control input*, denoted by u.

The only feature distinguishing the average model from the switched model will then be the control input. This will surely make things unequivocal.

The average model of the Buck converter is then described by

$$
\begin{aligned}
L\frac{di}{dt} &= -v + u_{av}E \\
C\frac{dv}{dt} &= i - \frac{v}{R}
\end{aligned}
\tag{2.4}
$$

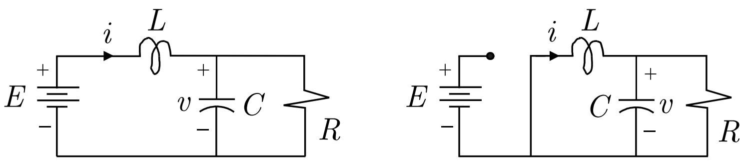

(a) Switch position at $u = 1$. (b) Switch position at $u = 0$.

Fig. 2.3. Circuit topologies in the Buck converter.

2.2.2 Normalization

Once the average model of the converter is obtained, we proceed to make some convenient changes in the scales measuring the magnitudes of the state variables and the time variable.

We define the new set of variables for the normalized system as follows:

$$
\begin{pmatrix} x_1 \\ x_2 \end{pmatrix} = \begin{pmatrix} \frac{1}{E}\sqrt{\frac{L}{C}} & 0 \\ 0 & \frac{1}{E} \end{pmatrix} \begin{pmatrix} i \\ v \end{pmatrix}, \qquad \tau = \frac{t}{\sqrt{LC}}
\tag{2.5}
$$

Note that the voltages in the system are being divided by the constant value of the external source voltage E. The normalized voltage of the source is therefore represented by 1. Using this state and input coordinate transformation on the average system (2.4) we readily obtain the *average normalized model* of the Buck converter

$$\begin{aligned} \frac{dx_1}{d\tau} &= -x_2 + u_{av} \\ \frac{dx_2}{d\tau} &= x_1 - \frac{x_2}{Q} \end{aligned} \tag{2.6}$$

where now the derivations in the left hand sides represent differentiations with respect to normalized (dimensionless) time τ. The variable x_1 is the normalized average current in the inductor L, x_2 is the normalized average output voltage and u_{av} represents the average switch position function, necessarily restricted to continuously take values on the set $[0, 1]$. The parameter Q is the inverse of the *quality factor of the circuit* and it is related to the resistance of the load by means of the relation: $Q = R\sqrt{C/L}$.

2.2.3 Equilibrium Point and Static Transfer Function

The control objective will be, most often, to regulate, the output voltage of the converter towards the desired average output voltage equilibrium value, taken as a constant reference signal. This is to be achieved by the application of an appropriate feedback control law u which will command the switch position in reference to an average value (this average value is most often interpreted as a *duty ratio* in a PWM scheme, but it may also be interpreted as an *equivalent control* in a sliding mode control scheme).

In general, it is desirable to relate the average values of the system variables, in steady state equilibrium, with the corresponding constant average value of the control input. These relations, also addressed as: *steady state relations* are useful in establishing the main *static* features of the converter.

In equilibrium, the time derivatives of the normalized average currents and voltages is set to zero while letting the average control input u_{av} to adopt a constant value $u_{av} = U$. As a result, we obtain a simple linear system of equations for the steady state equilibrium values of the average normalized state variables. Using the normalized average state representation (2.6) we obtain, denoting the average equilibrium values of the current and the output voltage as $\overline{x}_1$ and $\overline{x}_2$, the following relation:

$$\begin{pmatrix} 0 & 1 \\ 1 & -\frac{1}{Q} \end{pmatrix} \begin{pmatrix} \overline{x}_1 \\ \overline{x}_2 \end{pmatrix} = \begin{pmatrix} U \\ 0 \end{pmatrix} \tag{2.7}$$

Solving the system of equations for the unknowns $\overline{x}_1$ and $\overline{x}_2$, we obtain the equilibrium state of the system as:

$$\overline{x}_1 = \frac{1}{Q}U, \qquad \overline{x}_2 = U \tag{2.8}$$

This average control input parametrization of the equilibrium point is useful in establishing the "attenuation" characteristics of the converter. Indeed the average normalized output voltage exhibits the numerical value of the average control input U which is restricted to the interval $[0, 1]$. The average steady state output voltage is then restricted to such an interval. Since the normalized input voltage is fixed to the value of 1, this means that the output voltage will be only a fraction of the input voltage. The converter cannot "amplify" the input voltage.

The equilibrium state (2.8) can also be conveniently parameterized in terms of the desired equilibrium value of the output voltage. Suppose such a desired voltage is represented by V_d. We would then have, $\overline{x}_2 = V_d$, and thus,

$$\overline{x}_1 = \frac{1}{Q}V_d, \qquad \overline{x}_2 = V_d \tag{2.9}$$

We define the *normalized static transfer function* of the converter (also known as the *normalized converter gain*) as the normalized steady state normalized output voltage $\overline{x}_2$, written in terms of the constant average input U. We denote this quantity by $\mathcal{H}$ and, since it will be parameterized by the average input value U, we denote it by $\mathcal{H}(U)$. In the Buck converter case, it is given by the simple relation

$$\overline{x}_2 = \mathcal{H}(U) = U \tag{2.10}$$

In original coordinates, we can readily write the corresponding steady state relation by using (2.5). We define the *non-normalized static transfer function*, or simply the *static transfer function*, as the ratio of the steady state output voltage $\overline{v}$ and the constant input voltage E. We have

$$\frac{\overline{v}}{E} = \frac{UE}{E} = U = \mathcal{H}(U) \tag{2.11}$$

Clearly, the normalized and non-normalized static transfer functions are equivalent. Also, the maximum value of the gain is seen to be 1. For this reason, the Buck converter is sometimes addressed as the *voltage chopper*, or the *down converter*. The characteristic curve, corresponding to the value of the gain under feasible variations of the average control input equilibrium value U, is represented by a straight line as it is illustrated in Figure 2.4.

The equilibrium point for the actual state variables is obtained by inverting the transformation used in the normalization. This yields:

$$\overline{i} = \frac{1}{R}\overline{v}, \qquad \overline{v} = \overline{u}E \tag{2.12}$$

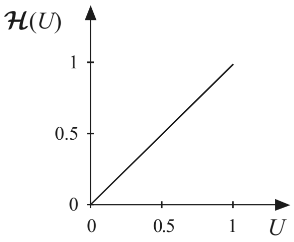

Fig. 2.4. Static transfer function of the Buck DC-to-DC power converter.

2.2.4 A Buck Converter Prototype

The Buck converter circuit, shown in Figure 2.1, was synthesized according to the diagram shown in Figure 2.5.

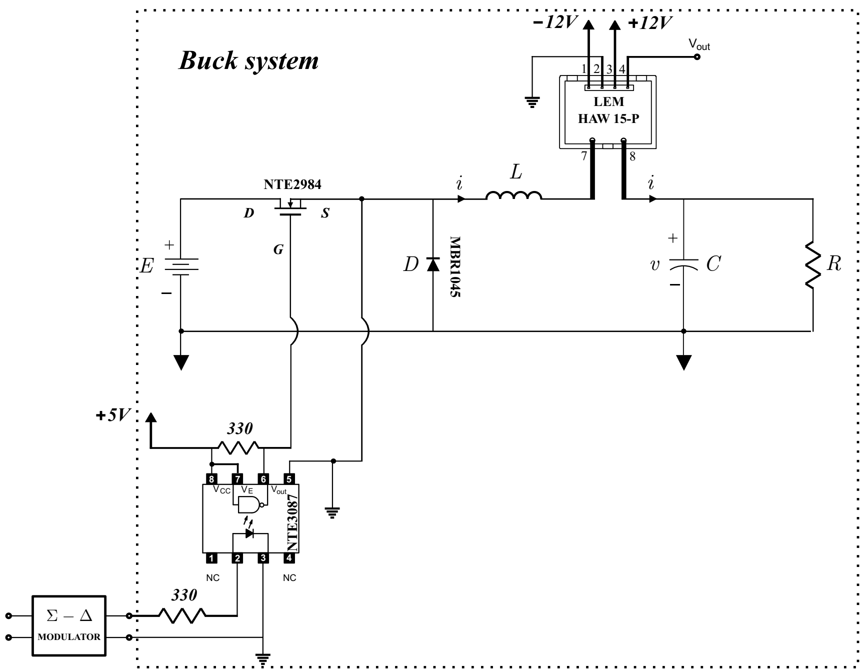

Fig. 2.5. Circuit diagram of the *Buck converter prototype.*

In this prototype circuit we will be implementing a feedback control law designed for the regulation of this system. The following parameters characterize the experimental test bed:

$$L = 15.91 \text{ mH}, \qquad C = 50 \ \mu\text{F}, \qquad R = 25 \ \Omega, \qquad E = 24 \text{ V}$$

The Buck converter was designed for an operation frequency of 45 kHz. The circuit diagram shown in Figure 2.5 illustrates the corresponding parts of the *Buck system*, while Figure 2.6 depicts a photograph of the actual circuit.

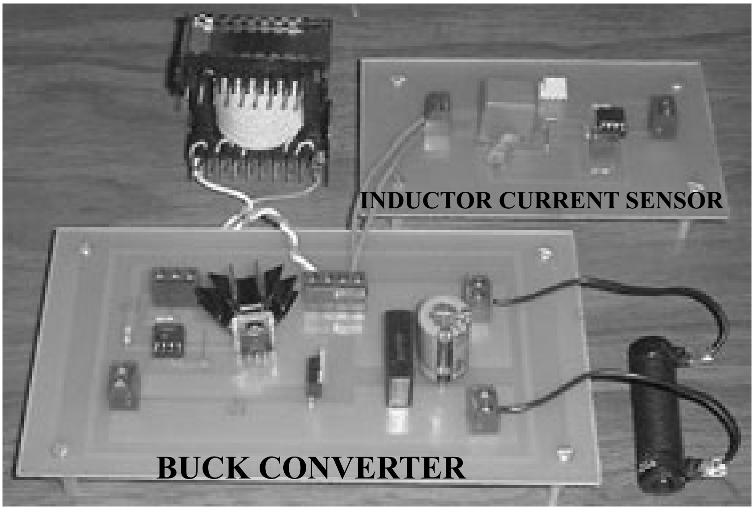

Fig. 2.6. Picture of the experimental Buck system.

According to Figure 2.5 we remark that the experimental *Buck converter prototype* consists of the following parts: *Buck system* (which includes the Buck converter, the *inductor current sensor*, the *capacitor voltage sensor* and the *driver*) and the *actuator*, represented by a $\Sigma - \Delta$-*modulator* or its corresponding *sliding mode* (SM) counterpart.

- *Buck system*: The core of this block is the Buck converter. The *inductor current sensor* consist of a LEM HAW 15-P sensor which operate under *Hall effect* principle. Additionally, the sensor bestows galvanic isolation between the Buck converter and the corresponding *control circuit*. The output voltage of the sensor is proportional to the inductor current i i.e., of the form ki. To obtain a relation 1 A : 1 V, we propose the circuit diagram shown in Figure 2.7. The *capacitor voltage sensor* let us obtain a measurement of the output voltage v. It consist of a voltage divisor so that we can reduce the amplitude of this signal in such a way that its final value is always in the 0-9 V interval. Figure 2.8 shows the voltage sensor. On the other hand, the *driver* is made up of the NTE3087 integrated circuit (IC). This circuit provides optical isolation between the *actuator* and the Buck converter. It also provides a suitably switching pulsed signal with amplitudes of 0 and 5 V, programmed to have a sampling rate of 45 kHz. The provided output signal allows to command the gate of a Mosfet (NTE2984) acting as a switch.

- $\Sigma - \Delta$-*modulator*: In this block the average synthesized control strategies are appropriately implemented in a switched manner. $\Sigma - \Delta$ modulation is a *sliding mode* based implementation technique which will be extremely useful in the actual realization of feedback control laws designed on the basis of average models. We present, at the end of Chapter 3 a detailed theoretical treatment of $\Sigma - \Delta$ modulation, and we also provide a proposal for the practical implementation of the $\Sigma - \Delta$-*modulator* which allows to limit the commutation frequency of the circuit to a finite value.

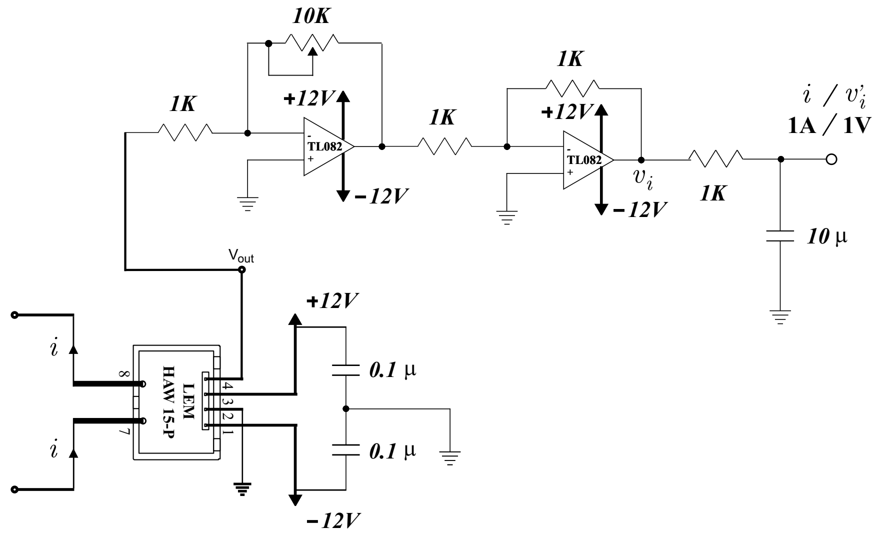

Fig. 2.7. Conditioning circuit for the inductor current measurement.

2.3 The Boost Converter

The electronic circuit of the Boost converter, also known as the *up converter*, is shown in Figure 2.9. We assume that the semi-conductors are ideal, i.e., the transistor Q has an infinitely fast response while the diode D has a threshold value equal to zero. This allows that the *conduction state* and the *blocking* states are activated with no loss of time whatsoever. From the preceding, we have the following behavior: when the transistor Q is in the *ON* state, the diode D is inversely polarized. As a consequence, there is no connection between the source voltage E and the system load R. This can be seen from

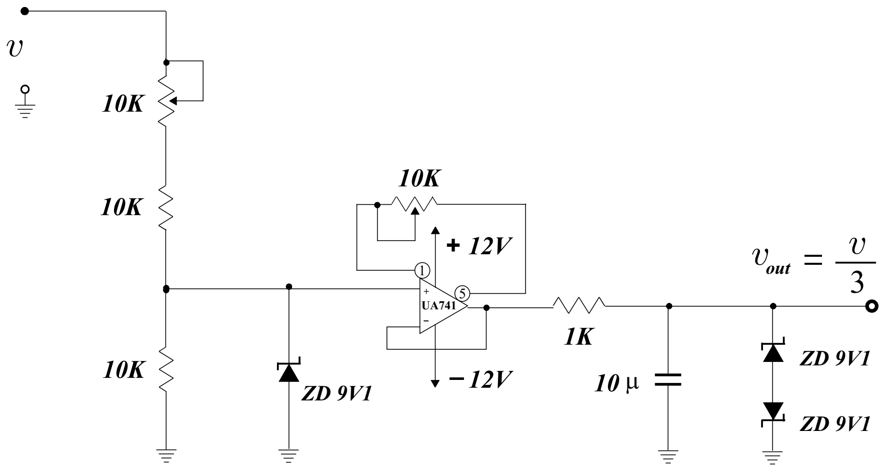

Fig. 2.8. Conditioning circuit for the capacitor voltage measurement.

the Figure 2.10(a). On the other hand, when the transistor Q is in the *OFF* state, the diode D is directly polarized, or D is conducting. This allows the flow of energy between the voltage source E and the load of the system R, as illustrated in Figure 2.10(b).

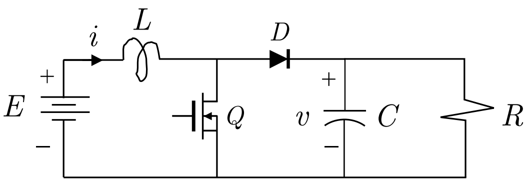

Fig. 2.9. Switched DC-to-DC power converter Boost using semi-conductor devices.

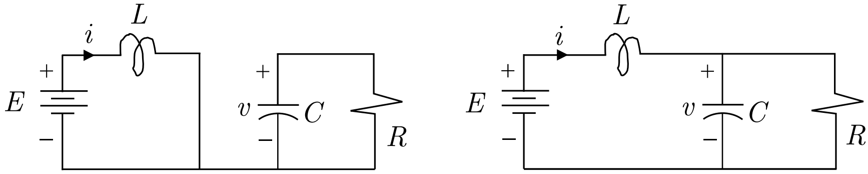

(a) The switch at the position $u = 1$. (b) The switch at the position $u = 0$.

Fig. 2.10. Circuit topologies involved in the Boost converter.

The two circuit topologies associated with the Boost converter (see Figure 2.10) may be combined into a single circuit diagram by means of the introduction of an ideal switch as shown in Figure 2.11.

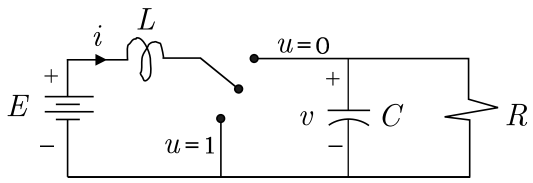

Fig. 2.11. DC-to-DC Boost converter with an ideal switch.

2.3.1 Model of the Converter

To obtain the dynamics of the Boost converter, we may apply Kirchoff's laws in each one of the circuit topologies arising as a consequence of the two switch positions. The first circuit topology is obtained when the switch position function is set to adopt the numerical value $u = 1$, and the second circuit topology is obtained when the switch position function takes the value $u = 0$. The two circuit topologies are shown in Figure 2.10.

When the switch position function is set to $u = 1$, we obtain, using Kirchoff's voltage and Kirchoff's current laws, the dynamics described by the following set of equations,

$$\begin{aligned} L\frac{di}{dt} &= E \\ C\frac{dv}{dt} &= -\frac{v}{R} \end{aligned} \tag{2.13}$$

When the switch position function is set to $u = 0$, we obtain the dynamics described by the equations,

$$\begin{aligned} L\frac{di}{dt} &= -v + E \\ C\frac{dv}{dt} &= i - \frac{v}{R} \end{aligned} \tag{2.14}$$

The Boost converter dynamics is then described by the following *bilinear* [1] type of system:

[1] We say that a system is *bilinear* when it is, independently, linear in the control u and linear in the state variables x, but not in both. In other words, the dynamics contains as nonlinearities, only the products of the form $x_i u$.

$$L\frac{di}{dt} = -(1-u)\,v + E$$
$$C\frac{dv}{dt} = (1-u)\,i - \frac{v}{R} \tag{2.15}$$

2.3.2 Normalization

The *normalization* of the Boost converter system equations is carried out by redefining the state variables and the time variable as follows:

$$\begin{pmatrix} x_1 \\ x_2 \end{pmatrix} = \begin{pmatrix} \frac{1}{E}\sqrt{\frac{L}{C}} & 0 \\ 0 & \frac{1}{E} \end{pmatrix} \begin{pmatrix} i \\ v \end{pmatrix}, \qquad \tau = \frac{t}{\sqrt{LC}} \tag{2.16}$$

We obtain the following *average normalized model* for the Boost converter,

$$\frac{dx_1}{d\tau} = -(1-u_{av})\,x_2 + 1$$
$$\frac{dx_2}{d\tau} = (1-u_{av})\,x_1 - \frac{x_2}{Q} \tag{2.17}$$

where the parameter Q, representing the inverse of a circuit quality factor, is obtained by the relation: $Q = R\sqrt{C/L}$. The variable x_1 is the normalized inductor current while x_2 represents the normalized output voltage. The switch position function is invariant with respect to the normalization process.

2.3.3 Equilibrium Point and Static Transfer Function

One of the control objectives, which we desire to achieve when using or designing a DC-to-DC power converter, is to regulate the output voltage so as to stabilize it to a constant value or to track a given reference signal. In the case of stabilization it becomes quite important to understand the steady state behavior of the circuit.

In the steady state regime, corresponding to constant equilibrium values, all time derivatives of the state variables in the description of the system are set to zero. Thus, the control input must also remain constant, i.e., $u_{av} = U = constant$. This condition results in a set of simultaneous equations whose solutions describe the equilibrium points of the system.

The normalized average model of the Boost converter corresponding to a constant value of the control input $u_{av} = U$, generates the following system of equations for the equilibrium states:

$$\begin{pmatrix} 0 & (1-U) \\ (1-U) & -\frac{1}{Q} \end{pmatrix} \begin{pmatrix} \overline{x}_1 \\ \overline{x}_2 \end{pmatrix} = \begin{pmatrix} 1 \\ 0 \end{pmatrix} \tag{2.18}$$

The solution of this system of equations for the steady state equilibrium values: $\overline{x}_1$ and $\overline{x}_2$ is given by

$$\overline{x}_1 = \frac{1}{Q}\frac{1}{(1-U)^2}, \qquad \overline{x}_2 = \frac{1}{(1-U)} \tag{2.19}$$

A different parametrization is obtained by expressing the equilibrium value in terms of the desired average output voltage of the converter, denoted by $\overline{x}_2 = V_d$:

$$\overline{x}_1 = \frac{1}{Q}V_d^2, \qquad \overline{x}_2 = V_d, \qquad U = \frac{V_d - 1}{V_d} \tag{2.20}$$

In this manner, from the relation (2.19), it is clear that the *static normalized transfer function* of the Boost converter is given by:

$$\mathcal{H}(U) = \overline{x}_2 = \frac{1}{(1-U)} \tag{2.21}$$

It is clear that the gain of the converter circuit is always larger than 1. For this reason, this converter is addressed as the *up converter* or the *Boost converter.* The *characteristic curve* of the *static transfer function* for the Boost converter is depicted in Figure 2.12. It is clear that through the variation of the *duty cycle* or *average control input* U, we can read the actual steady state output voltage of desired value $\overline{v}$ provided it is larger than 1.

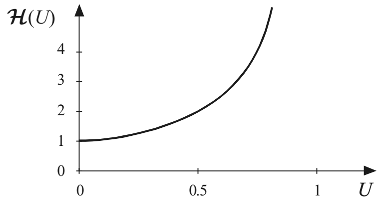

Fig. 2.12. Characteristic curve of the static transfer function of the Boost DC-to-DC power converter.

The equilibrium values of the non-normalized Boost power converter state variables are obtained as:

$$\overline{i} = \frac{1}{R}\frac{\overline{v}^2}{E}, \qquad \overline{v} = \frac{E}{(1-U)} \tag{2.22}$$

2.3.4 Alternative Model of the Boost Converter

It is important to notice that the switch position function values $u = 1$ and $u = 0$ of the Buck and Boost power converters can be realized in a non-unique form, i.e., any of the ideal switch positions can be made to correspond with, say, the value $u = 1$. In general, it is more convenient to assign the position function value $u = 1$ to that corresponding to the *conducting mode* for the power transistor Q. As a consequence, the other position function value, $u = 0$, corresponds to the power transistor Q being in the *non-conducting mode.* This is a natural convention that will be adopted in this chapter. However, in the following chapters, we will also use the alternative model for some of the converters, in particular for the *Boost converter.* The alternative models may be of significant help in the algebraic manipulations for the derivation of the various controller schemes. Thus, the alternative model for the normalized average model of the Boost converter (2.17) is given by:

$$\begin{aligned} \frac{dx_1}{d\tau} &= -\mathbf{u}_{av} x_2 + 1 \\ \frac{dx_2}{d\tau} &= \mathbf{u}_{av} x_1 - \frac{1}{Q} x_2 \end{aligned} \tag{2.23}$$

where clearly, the new control input $\mathbf{u}_{av}$ satisfies,

$$\mathbf{u}_{av} = 1 - u_{av} \tag{2.24}$$

2.3.5 A Boost Converter Prototype

Figure 2.13 shows the circuit diagram of a *Boost converter prototype.* The circuit parameters adopted for this experimental system are given by:

$$L = 15.91 \text{ mH}, \qquad C = 50\ \mu\text{F}, \qquad R = 52\ \Omega, \qquad E = 12 \text{ V}$$

where the inductor L was designed to operate at 45 kHz. Figure 2.14 depicts a picture of the actual *Boost system.* Similar to the *Buck converter prototype*, the *Boost converter prototype* is made up of two blocks: *Boost system* and a $\Sigma - \Delta$*-modulator*, or its corresponding SM counterpart, acting as an *actuator.*

- *Boost system*: It is made up of four circuits: 1) a Boost converter, 2) an *inductor current sensor*, 3) a *capacitor voltage sensor* and 4) a *driver.* The *inductor current sensor* was chosen to be a LEM HAW 15-P. The conditioning circuits for the inductor current and capacitor voltage measurements are the same that we employed for the *Buck system.* These circuits are shown in Figure 2.7 and Figure 2.8, respectively. On the other hand, the *driver* is made up of an NTE3087 IC. The NTE3087 IC provides optical isolation between the $\Sigma - \Delta$*-modulator* and the Boost converter circuit. It provides a suitably switching pulsed signal with amplitudes restricted to 0 and 5 V. It is programmed to sustain a sampling rate of 45 kHz. The provided output signal allows to command the gate of the Mosfet NTE2984, which acts as the switch (see Figure 2.13).
- $\Sigma - \Delta$*-modulator*: In this block, the control strategies, designed on the basis of average models, are appropriately implemented.

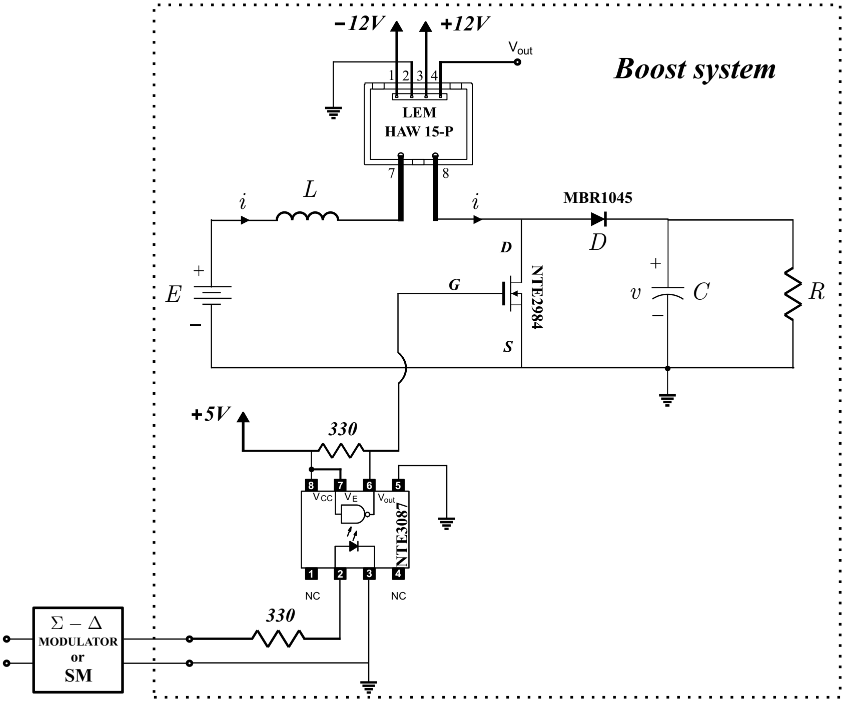

Fig. 2.13. Circuit diagram for the experimental *Boost converter prototype.*

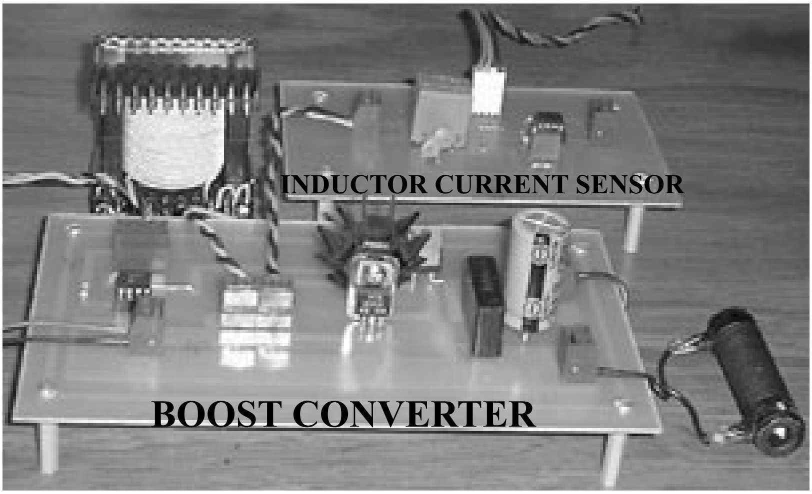

Fig. 2.14. Photograph of the experimental Boost system.

2.4 The Buck-Boost Converter

Another possible arrangement of the semiconductor switches, gives room to a third type of DC-to-DC power converter known as the Buck-Boost converter. In fact, this new converter is obtained by interchanging the diode D and the inductor L of the Buck converter. The circuit is shown in Figure 2.15. This converter is also known as the *chopper-amplifier converter*. In this type of converter, the circuit gain may be higher or lower than 1 modulo a polarity change. The fundamental difference of this class of converter with the Buck and the Boost converters is that the output voltage is of *opposite sign* to that of the constant source E.

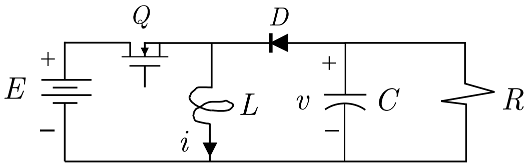

Fig. 2.15. Buck-Boost converter with semiconductor switch realization.

Assuming that the Buck-Boost circuit components are ideal, the resulting circuit is the one shown in Figure 2.16, where the semiconductors (Q, D) have been substituted by an ideal switch.

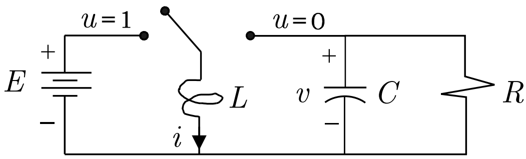

Fig. 2.16. Ideal switch representation of the Buck-Boost DC-to-DC converter.

2.4.1 Model of the Converter

The operation of this system is as follows: when the transistor is switched to the ON state (conduction state), the diode is inversely polarized generating a circuit topology which is shown in Figure 2.17(a). During this period, the inductor current is generated from the source voltage E. While the diode remains inversely polarized we say the circuit is operating in the "charging period". When the transistor is switched OFF, the diode is directly polarized generating the circuit topology shown in Figure 2.17(b). This second period is known as the “discharging period” due to the fact that the stored energy in the inductor L is transferred to the system load R.

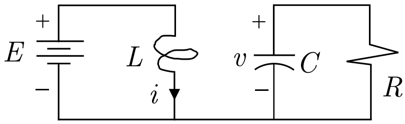

(a) Switch position at $u = 1$.

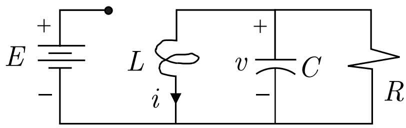

(b) Switch position at $u = 0$.

Fig. 2.17. Circuits topologies associated with the Buck-Boost converter.

When the Kirchoff’s voltage and current laws are applied to the two circuit topologies of Figure 2.17, and the obtained models are combined into a single dynamic model, the resulting system of differential equations describing the Buck-Boost converter is the following:

$$
\begin{aligned}
L\frac{di}{dt} &= (1-u)\,v + uE \\
C\frac{dv}{dt} &= -\,(1-u)\,i - \frac{v}{R}
\end{aligned}
\tag{2.25}
$$

2.4.2 Normalization

The *average normalized model* of the Buck-Boost converter is given by

$$
\begin{aligned}
\frac{dx_1}{d\tau} &= (1-u_{av})\,x_2 + u_{av} \\
\frac{dx_2}{d\tau} &= -\,(1-u_{av})\,x_1 - \frac{x_2}{Q}
\end{aligned}
\tag{2.26}
$$

where the variable x_1 represents the normalized inductor current, x_2 is the normalized output voltage and u_{av}, represents, as before, the average control variable.

Clearly the underlying transformation is, just as before, given by

$$
\begin{pmatrix} x_1 \\ x_2 \end{pmatrix} = \begin{pmatrix} \frac{1}{E}\sqrt{\frac{L}{C}} & 0 \\ 0 & \frac{1}{E} \end{pmatrix} \begin{pmatrix} i \\ v \end{pmatrix}, \qquad Q = R\sqrt{C/L}, \qquad \tau = \frac{t}{\sqrt{LC}}
\tag{2.27}
$$

Similarly as in the Boost converter case, we can justify the use of the following alternative model for the Buck-Boost converter,

$$
\begin{aligned}
\frac{dx_1}{d\tau} &= \mathbf{u}_{av}x_2 + (1-\mathbf{u}_{av}) \\
\frac{dx_2}{d\tau} &= -\mathbf{u}_{av}x_1 - \frac{1}{Q}x_2
\end{aligned}
\tag{2.28}
$$

where

$$\mathbf{u}_{av} = 1 - u_{av} \tag{2.29}$$

2.4.3 Equilibrium Point and Static Transfer Function

The equilibrium point of the Buck-Boost corresponding to a constant value of the average control input is obtained by letting the right hand side of the state equations (2.26) to be zero while the control variable is set to be $u_{av} = U =$ *constant*. We thus obtain a system of equations for $\overline{x}_1$ and $\overline{x}_2$ given by

$$\begin{pmatrix} 0 & (1-U) \\ -(1-U) & -\frac{1}{Q} \end{pmatrix} \begin{pmatrix} \overline{x}_1 \\ \overline{x}_2 \end{pmatrix} = \begin{pmatrix} -U \\ 0 \end{pmatrix} \tag{2.30}$$

The equilibrium point of the Buck-Boost converter parameterized in terms of the constant value U of the control input is then given by,

$$\overline{x}_1 = \frac{1}{Q}\frac{U}{(1-U)^2}, \qquad \overline{x}_2 = -\frac{U}{(1-U)} \tag{2.31}$$

The equilibrium point, parameterized now in terms of the desired constant normalized average output voltage $\overline{x}_2 = V_d$, is given by the following relations:

$$\overline{x}_1 = (V_d - 1)\frac{V_d}{Q}, \qquad \overline{x}_2 = V_d, \qquad U = \frac{V_d}{V_d - 1} \tag{2.32}$$

On the other hand, the actual (or de-normalized) steady state variables corresponding to the equilibrium point (2.32) are obtained when we introduce the redefining state variables (2.27) into (2.32), generating:

$$\overline{i} = \left(\frac{\overline{v}}{E} - 1\right)\frac{\overline{v}}{R}, \qquad \overline{v} = -\left(\frac{U}{1-U}\right)E \tag{2.33}$$

The *normalized static transfer function* of the Buck-Boost converter is immediately obtained from Equation 2.31 as:

$$\mathcal{H}(U) = -\frac{U}{(1-U)} \tag{2.34}$$

The graph in Figure 2.18 depicts the *static transfer function* of the Buck-Boost converter. It is also clear that we may read the steady state output voltage of the system $\overline{v}$, in correspondence with the average control input equilibrium value U. It is also clear from the characteristic curve of the Buck-Boost converter that this circuit may either amplify, or reduce, the constant input voltage but with the output voltage polarity being opposite to that of the system constant input voltage source E.

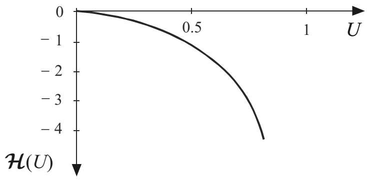

Fig. 2.18. Characteristic curve of the Buck-Boost DC-to-DC power converter.

2.4.4 A Buck-Boost Converter Prototype

The circuit schematics, the actual circuit, as well as a picture of the prototype for the *Buck-Boost system* are shown in Figures 2.15, 2.19, and 2.20, respectively. The values of the components for this system were set to be:

$$L = 15.91 \text{ mH}, \qquad C = 470 \ \mu\text{F}, \qquad R = 52 \ \Omega, \qquad E = 12 \text{ V}$$

The switching frequency for this converter, as in the previous converters, is 45 kHz.

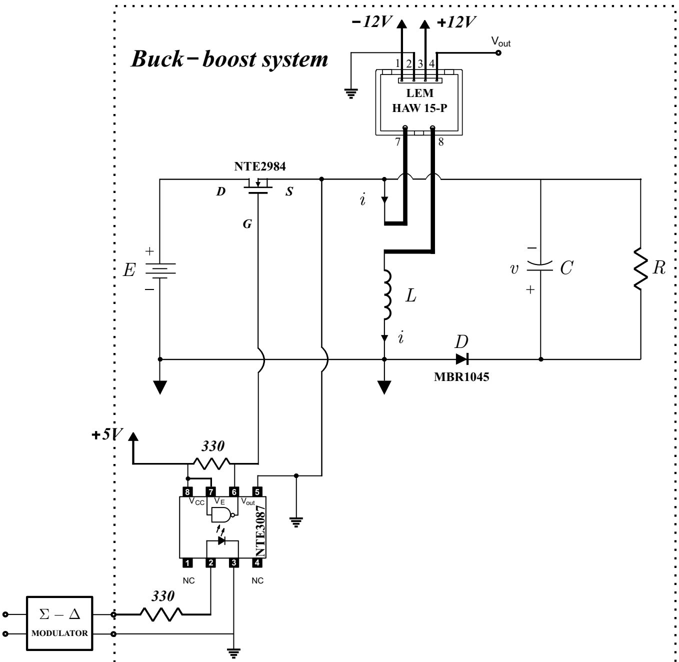

Fig. 2.19. Circuit of the *Buck-Boost converter prototype.*

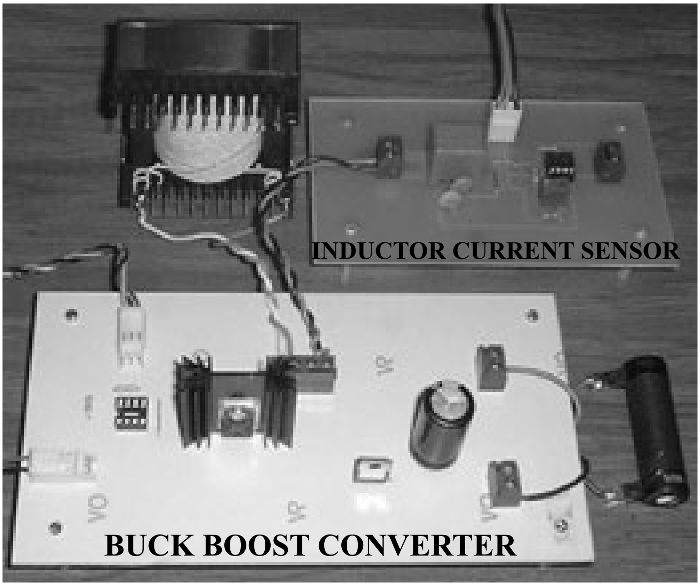

Fig. 2.20. Hardware implementation of the Buck-Boost system.

2.5 The Non-inverting Buck-Boost Converter

Our main objective in the previous section was centered around the study of the DC-to-DC Buck-Boost converter, which exhibited the particular property of delivering an output voltage of opposite polarity with respect to that of the input voltage source E along with the possibility of amplifying or scaling down this value. Following the same presentation scheme used in the previous section, we shall now deal with the non-inverting Buck-Boost converter. This converter also has the capability of scaling and of amplifying the constant input voltage source value E at the output. The fundamental difference is that this new converter does not change the polarity of the input voltage source E at the output.

2.5.1 Model of the Converter

The configuration of the non-inverting Buck-Boost converter, assuming that the circuit components are all ideal, is shown in Figure 2.21.

If we consider the ideal switch version of the converter, shown in Figure 2.21, the model of the system may be directly obtained using the same procedure as in the previous examples.

The dynamics describing to the non-inverting Buck-Boost converter is found to have the following state representation:

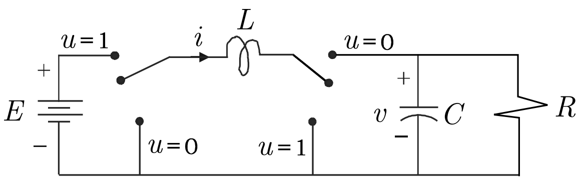

Fig. 2.21. Simplified non-inverting Buck-Boost converter.

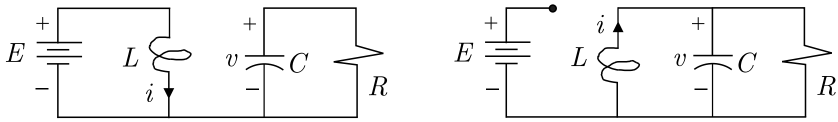

(a) Switch position at $u = 1$. (b) Switch position at $u = 0$.

Fig. 2.22. Circuit topologies involved in the non-inverting Buck-Boost converter.

$$\begin{aligned} L\frac{di}{dt} &= -\left(1-u\right)v + uE \\ C\frac{dv}{dt} &= \left(1-u\right)i - \frac{v}{R} \end{aligned} \tag{2.35}$$

where i and v are, respectively, the current through the inductor L and the voltage across the terminals of the capacitor C. The external source voltage E has a constant value. The variable u is the control input, which represents the switch position, restricted to take values in the discrete set $\{0, 1\}$. The control objective consists in regulating the output voltage v around a desired equilibrium point.

2.5.2 Normalization

Using precisely the same state coordinate transformation and time scaling used in the three previous cases, the normalized model of the non-inverting Buck-Boost converter is written as,

$$\begin{aligned} \dot{x}_1 &= -\left(1-u\right)x_2 + u \\ \dot{x}_2 &= \left(1-u\right)x_1 - \frac{x_2}{Q} \end{aligned} \tag{2.36}$$

With some abuse of notation we use " $\cdot$ " to denote the derivative with respect to the dimensionless time τ. The normalized variables x_1 y x_2 represent, respectively, the normalized current and the normalized output voltage. The switch position function is still represented by u. The only remaining parameter in the normalized model, Q, is expressed as,

$$Q = R\sqrt{\frac{C}{L}} \tag{2.37}$$

2.5.3 Equilibrium Point and Static Transfer Function

The equilibrium point of the average non-inverting Buck-Boost converter is obtained from the solution of the corresponding set of algebraic equations when u_{av} is set to be the constant value U and the time derivatives of the normalized state variables is set to zero. We obtain,

$$\overline{x}_1 = \frac{1}{Q}\frac{U}{(1-U)^2}, \qquad \overline{x}_2 = \frac{U}{(1-U)} \tag{2.38}$$

Using these expressions, we may rewrite the normalized value of the equilibrium inductor current $\overline{x}_1$ in terms of the normalized output voltage $\overline{x}_2$ as follows:

$$\overline{x}_1 = (\overline{x}_2 + 1)\,\frac{\overline{x}_2}{Q} \tag{2.39}$$

Thus, if we wish to regulate the normalized output voltage x_2 towards a desired equilibrium value $\overline{x}_2$, then, this may be achieved in an indirect fashion by regulating the variable x_1 towards its corresponding equilibrium value given by (2.39).

According to (2.38) the normalized *gain* for the non-inverting Buck-Boost converter is given by:

$$\mathcal{H}(U) = \overline{x}_2 = \frac{U}{(1-U)} \tag{2.40}$$

From here, we may confirm that, in steady state, the non-inverting Buck-Boost converter may either *attenuate*, or *rise*, at the output terminals, the constant *input voltage* E. Moreover, this is achieved without polarity inversion with respect to the input source E.

The graph of the corresponding characteristic curve for this converter system is shown in Figure 2.23.

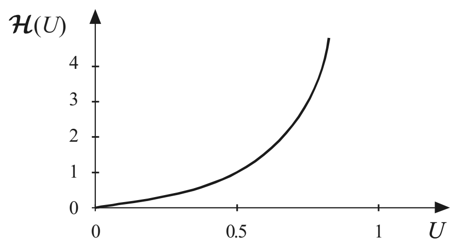

Fig. 2.23. Characteristic curve for the non-inverting Buck-Boost converter.

2.6 The Cúk Converter

By suitable combination of some of the basic converter topologies representing the Buck, the Boost and the Buck-Boost converters, one may obtain some other useful DC-to-DC power converters. A typical example is the cascade connection of the Boost and the Buck converter which produces the well known Cúk converter. This converter is shown in Figure 2.24. The input circuit in the Cúk converter is, clearly, a Boost, converter and the output circuit is seen to be a Buck converter. Thus, we may also think of the Cúk converter as a "*Boost-Buck*" converter. In contradistinction to the basic topologies, the Cúk converter requires two (dependent) switches instead of one as well as two inductors L_1, L_2, and two capacitors; one for storing the energy and the second one to transfer the energy from the input circuit towards the output circuit load. This results in a higher complexity for the analysis and construction of the converter. The *static transfer function* of the Cúk converter exhibits the same characteristic curve we obtained for the Buck-Boost converter, as it will be shown in this section.

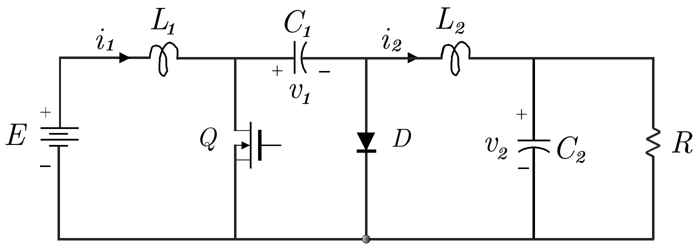

Fig. 2.24. Practical Cúk converter realization.

The ideal switch (and ideal components) circuit diagram for the Cúk converter is shown in Figure 2.24. This idealization may be contrasted against a practical realization of the Cúk converter, shown in Figure 2.25. This simplified circuit representation will allow us to obtain, rather directly, the dynamic model of the converter.

The Cúk converter exhibits two different modes of operation. The first mode is obtained when the transistor is ON and instantaneously, the diode D is inversely polarized generating an circuit topology shown in Figure 2.26(a). During this period, the current through the inductor L_1 is drawn from the voltage source E. This mode represents the *charging* mode. The second mode of operation starts when the transistor is OFF and the diode D is directly polarized generating the circuit topology shown in Figure 2.26(b). This stage or mode of operation is known as the *discharging* mode since all the energy stored in L_1 is now transferred to the load R.

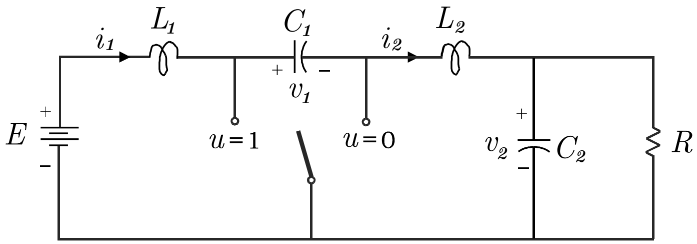

Fig. 2.25. Ideal switch representation of the Cúk converter.

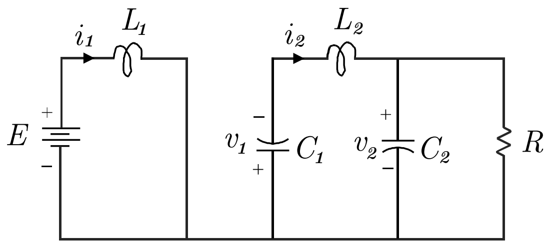

(a) Switch position at $u = 1$.

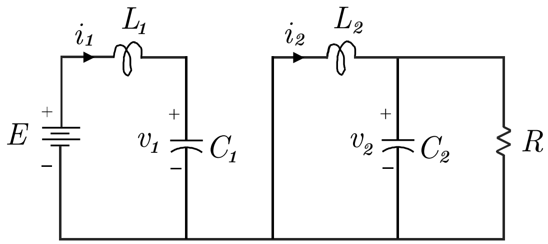

(b) Switch position at $u = 0$.

Fig. 2.26. Equivalent circuits of the Cúk converter.

2.6.1 Model of the Converter

The derivation of the dynamics of the *Cúk* converter is carried out in the same manner in which we analyzed the topologies of the previous basic DC-to-DC power converters.

When $u = 1$, we obtain the following equations for i_1 and i_2 in the obtained circuit topology,

$$\begin{aligned} L_1 \frac{di_1}{dt} &= E \\ L_2 \frac{di_2}{dt} &= -v_1 - v_2 \end{aligned} \tag{2.41}$$

and the following equations for the capacitor voltages v_1 and v_2,

$$C_1 \frac{dv_1}{dt} = i_2$$
$$C_2 \frac{dv_2}{dt} = i_2 - \frac{v_2}{R} \tag{2.42}$$

When $u = 0$, we obtain the following equations for i_1 and i_2,

$$L_1 \frac{di_1}{dt} = -v_1 + E$$
$$L_2 \frac{di_2}{dt} = -v_2 \tag{2.43}$$

The capacitor voltages v_1 and v_2 are described by,

$$C_1 \frac{dv_1}{dt} = i_1$$
$$C_2 \frac{dv_2}{dt} = i_2 - \frac{v_2}{R} \tag{2.44}$$

The *Cúk* converter dynamics is then described by combining the previous partial models. We obtain the following system of differential equations:

$$L_1 \frac{di_1}{dt} = -(1-u)\, v_1 + E$$
$$C_1 \frac{dv_1}{dt} = (1-u)\, i_1 + u i_2$$
$$L_2 \frac{di_2}{dt} = -u v_1 - v_2$$
$$C_2 \frac{dv_2}{dt} = i_2 - \frac{v_2}{R} \tag{2.45}$$

where v_1 and i_1 are, respectively, the voltage across the capacitor C_1 and the current in the inductor L_1, while v_2 and i_2 are, respectively, the voltage across the parallel branches formed by the capacitor C_2 and the load R, and the current through the inductor L_2. As usual, the external voltage source E has a constant value. The variable u is the control input, which represents the switch position restricted to take values in the discrete set $\{0, 1\}$. It is assumed that the converter operates in the *continuous conduction mode*, i.e., neither of the inductor currents are identically zero on an open interval of time.

2.6.2 Normalization

Once we have obtained the *Cúk* converter model, we proceed to perform the normalizing transformations of the state variable and time coordinates.

The state coordinates transformation and time scaling:

$$\begin{pmatrix} x_1 \\ x_2 \\ x_3 \\ x_4 \end{pmatrix} = \begin{pmatrix} \frac{1}{E}\sqrt{\frac{L_1}{C_1}} & 0 & 0 & 0 \\ 0 & \frac{1}{E} & 0 & 0 \\ 0 & 0 & \frac{1}{E}\sqrt{\frac{L_1}{C_1}} & 0 \\ 0 & 0 & 0 & \frac{1}{E} \end{pmatrix} \begin{pmatrix} i_1 \\ \upsilon_1 \\ i_2 \\ \upsilon_2 \end{pmatrix}, \qquad \tau = \frac{t}{\sqrt{L_1 C_1}} \tag{2.46}$$

yields the following normalized model for the Cúk converter:

$$\begin{aligned} \dot{x}_1 &= -(1-u)\,x_2 + 1 \\ \dot{x}_2 &= (1-u)\,x_1 + u x_3 \\ \alpha_1 \dot{x}_3 &= -u x_2 - x_4 \\ \alpha_2 \dot{x}_4 &= x_3 - \frac{x_4}{Q} \end{aligned} \tag{2.47}$$

where the symbol: " $\cdot$ " again represents (abusively) the derivative with respect to the dimensionless time coordinate τ. The variables x_1, x_3 and x_2, x_4 represent, respectively, the currents and the voltages of the normalized system, while u represents the switch position function. The parameter Q is defined as $Q = R\sqrt{C_1/L_1}$, while the constants α_1 and α_2 are defined by the quotients

$$\alpha_1 = L_2/L_1, \qquad \alpha_2 = C_2/C_1 \tag{2.48}$$

2.6.3 Equilibrium Point and Static Transfer Function

Setting to zero the right hand sides of the average normalized model (2.47) with $u_{av} = U = constant$, yields the following system of equations:

$$\begin{pmatrix} 0 & -(1-U) & 0 & 0 \\ 1-U & 0 & U & 0 \\ 0 & -U & 0 & -1 \\ 0 & 0 & 1 & -\frac{1}{Q} \end{pmatrix} \begin{pmatrix} \overline{x}_1 \\ \overline{x}_2 \\ \overline{x}_3 \\ \overline{x}_4 \end{pmatrix} = \begin{pmatrix} -1 \\ 0 \\ 0 \\ 0 \end{pmatrix} \tag{2.49}$$

whose solution is found to be given by:

$$\overline{x}_1 = \frac{1}{Q}\frac{U^2}{(1-U)^2}, \qquad \overline{x}_2 = \frac{1}{1-U}, \qquad \overline{x}_3 = -\frac{1}{Q}\frac{U}{(1-U)}, \qquad \overline{x}_4 = -\frac{U}{1-U} \tag{2.50}$$

A different parametrization of the equilibria is obtained by using a constant desired value of the output voltage $\overline{x}_4$. Such a parametrization is given by:

$$\overline{x}_1 = \frac{\overline{x}_4^2}{Q}, \qquad \overline{x}_2 = 1 - \overline{x}_4, \qquad \overline{x}_3 = \frac{\overline{x}_4}{Q}, \qquad U = \frac{\overline{x}_4}{\overline{x}_4 - 1} \tag{2.51}$$

From the relation existing between the constant output voltage of the converter, $\overline{x}_4$ and the corresponding value of the average control input U, determined in (2.50), the *static normalized transfer function* of the Cúk converter is readily found to be

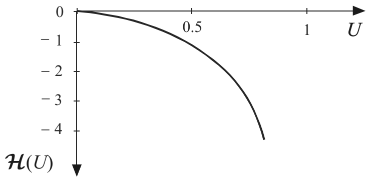

Fig. 2.27. Characteristic curve of the static transfer function of the Cúk DC-to-DC power converter.

$$\mathcal{H}(U) = \overline{x}_4 = -\frac{U}{(1-U)} \tag{2.52}$$

The characteristic curve of the *static transfer function* of the Cúk converter is shown in Figure 2.27. As it was previously stated, the characteristic curve of the voltage gain of the Cúk converter is the same as that of the Buck-Boost converter.

2.7 The Sepic Converter

Figure 2.28 shows the Sepic DC-to-DC converter circuit with switches realized by means of semiconductor devices(Q, D). These operate in a complementary fashion i.e., when the transistor Q is in the conducting mode then the diode D is inversely polarized and viceversa.

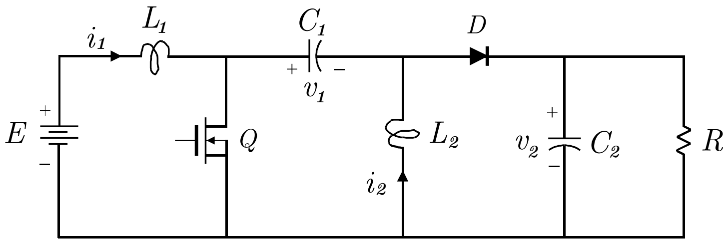

Fig. 2.28. The Sepic DC-to-DC power converter.

Figure 2.29 depicts the ideal switch realization of the Sepic converter. The equivalent circuits, corresponding to the switch position function values, $u = 1$ and $u = 0$, are shown in Figure 2.30

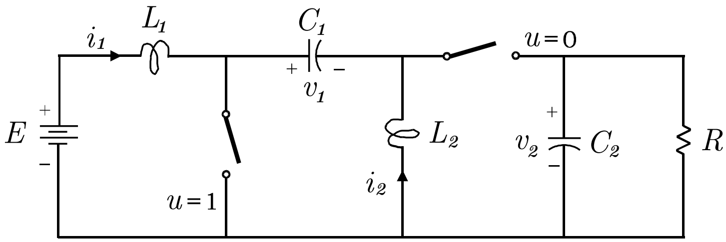

Fig. 2.29. Sepic converter realization with ideal switches.

2.7.1 Model of the Converter

The model of the converter is derived to be:

$$\begin{aligned}
L_1 \frac{di_1}{dt} &= -(1-u)(v_1+v_2)+E \\
C_1 \frac{dv_1}{dt} &= (1-u)\, i_1 - u i_2 \\
L_2 \frac{di_2}{dt} &= u v_1 - (1-u)\, v_2 \\
C_2 \frac{dv_2}{dt} &= (1-u)(i_1+i_2) - \frac{v_2}{R}
\end{aligned} \tag{2.53}$$

where v_1 and i_1 are, respectively, the voltage across capacitor C_1 and the current through the inductor L_1, v_2 and i_2 are, respectively, the voltage across the capacitor C_2 and the load R, and the inductor current L_2. The source voltage E is constant. The control input u is the switch position function taking values in $\{0, 1\}$.

2.7.2 Normalization

The following state coordinate transformation and time scaling,

$$\begin{pmatrix} x_1 \\ x_2 \\ x_3 \\ x_4 \end{pmatrix} = \begin{pmatrix} \frac{1}{E}\sqrt{\frac{L_1}{C_1}} & 0 & 0 & 0 \\ 0 & \frac{1}{E} & 0 & 0 \\ 0 & 0 & \frac{1}{E}\sqrt{\frac{L_1}{C_1}} & 0 \\ 0 & 0 & 0 & \frac{1}{E} \end{pmatrix} \begin{pmatrix} i_1 \\ v_1 \\ i_2 \\ v_2 \end{pmatrix}, \qquad \tau = \frac{t}{\sqrt{L_1 C_1}} \tag{2.54}$$

yields the following normalized model of the Sepic converter:

$$\begin{aligned}
\dot{x}_1 &= -(1-u)(x_2+x_4)+1 \\
\dot{x}_2 &= (1-u)\, x_1 - u x_3 \\
\alpha_1 \dot{x}_3 &= u x_2 - (1-u)\, x_4 \\
\alpha_2 \dot{x}_4 &= (1-u)(x_1+x_3) - \frac{x_4}{Q}
\end{aligned} \tag{2.55}$$

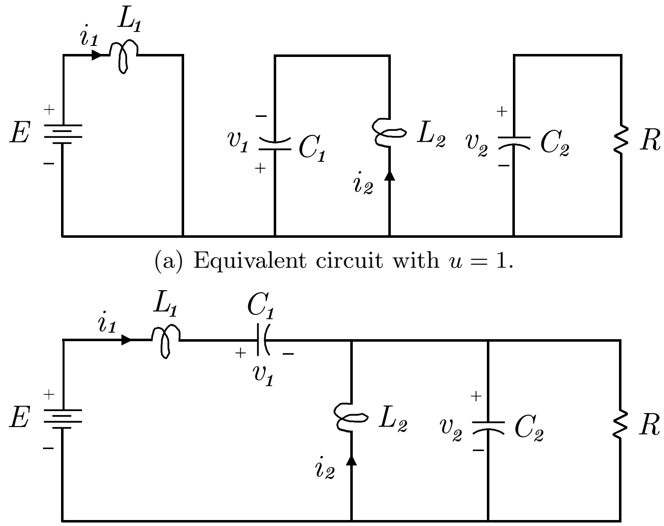

(a) Equivalent circuit with $u = 1$.

(b) Equivalent circuit with $u = 0$.

Fig. 2.30. Circuit topologies associated with the Sepic converter.

The constants α_1, α_2 and Q are defined by:

$$\alpha_1 = L_2/L_1, \qquad \alpha_2 = C_2/C_1, \qquad Q = R\sqrt{C_1/L_1} \tag{2.56}$$

2.7.3 Equilibrium Point and Static Transfer Function

The normalized average state equilibrium point, parameterized in terms of the constant average input U, is readily obtained as

$$\overline{x}_1 = \frac{1}{Q}\frac{U^2}{(1-U)^2}, \qquad \overline{x}_2 = 1, \qquad \overline{x}_3 = \frac{1}{Q}\frac{U}{(1-U)}, \qquad \overline{x}_4 = \frac{U}{(1-U)} \tag{2.57}$$

Parameterizing the equilibrium values in terms of the constant output voltage $\overline{x}_4$ leads to:

$$\overline{x}_1 = \frac{\overline{x}_4^2}{Q}, \qquad \overline{x}_2 = 1, \qquad \overline{x}_3 = \frac{\overline{x}_4}{Q}, \qquad U = \frac{\overline{x}_4}{\overline{x}_4 + 1} \tag{2.58}$$

The *static transfer function* is obtained to be:

$$\mathcal{H}(U) = \overline{x}_4 = \frac{U}{(1-U)} \tag{2.59}$$

which points to the fact that the Sepic converter can *reduce* or *amplify*, in steady state, the constant input source voltage value. Clearly, the output voltage is of the same polarity as that of the source input E. Figure 2.31 shows the corresponding characteristic curve.

The equilibrium point for the actual state variables is obtained by inverting the transformation used in the normalization. This yields:

$$\bar{i}_1 = \frac{1}{R}\frac{\overline{v}_2^2}{E}, \qquad \overline{v}_1 = E, \qquad \bar{i}_2 = \frac{\overline{v}_2}{R}, \qquad \overline{v}_2 = \frac{U}{(1-U)}E \tag{2.60}$$

where,

$$U = \frac{\overline{v}_2}{\overline{v}_2 + E} \tag{2.61}$$

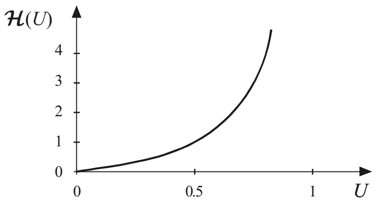

Fig. 2.31. Characteristic curve for the Sepic DC-to-DC power converter.

2.8 The Zeta Converter

Similarly to the Cúk and the Sepic converters, the Zeta converter may be represented by a fourth order nonlinear (bilinear) system. The reason being is that it includes two capacitors and two inductors as dynamic storage elements. The Zeta converter can both amplify and reduce, without polarity inversions, the value of the input source voltage E. We briefly summarize next the most important features involved in the modelling of the Zeta converter.

Figure 2.32 depicts a semiconductor realization of a Zeta DC-to-DC power converter. The ideal switch based realization of the Zeta converter is depicted in Figure 2.33.

2.8.1 Model of the Converter

The Zeta converter exhibits two different modes of operation. The first mode is obtained when the transistor is ON and instantaneously, the diode D is inversely polarized generating an equivalent circuit shown in Figure 2.34(a). During this period, the current through the inductor L_1 and L_2 are drawn from the voltage source E. This mode is the *charging* mode. The second mode of operation starts when the transistor is OFF and the diode D is directly

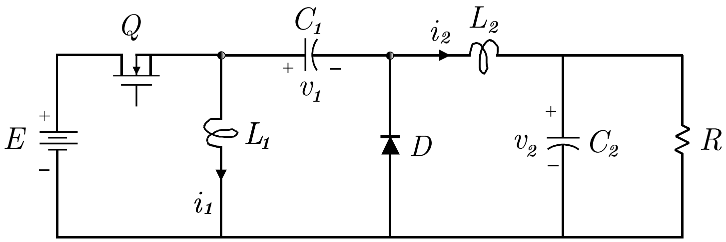

Fig. 2.32. A Zeta converter using a semiconductor realization of the switches.

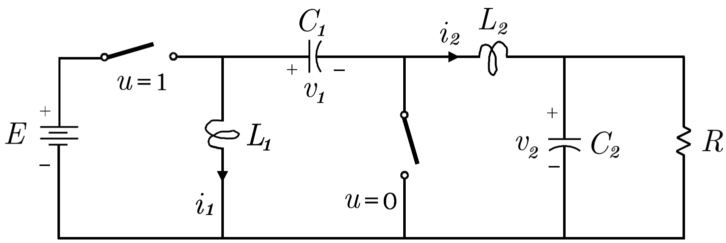

Fig. 2.33. The Zeta converter with ideal switches.

polarized generating the equivalent circuit shown in Figure 2.34(b). This stage or mode of operation is known as the *discharging* mode since all the energy stored in L_2 is now transferred to the load R.

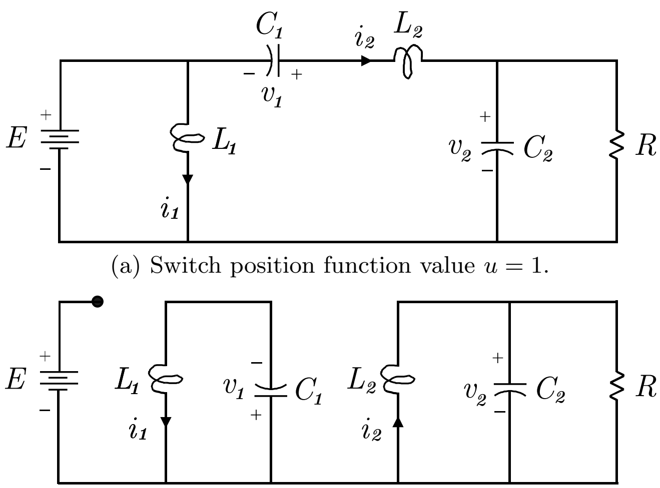

(a) Switch position function value $u = 1$.

(b) Switch position function value $u = 0$.

Fig. 2.34. Circuit topologies associated with the Zeta converter.

The dynamical model of the Zeta converter is found to be

$$
\begin{aligned}
L_1 \frac{di_1}{dt} &= -(1-u)\,\upsilon_1 + uE \\
C_1 \frac{d\upsilon_1}{dt} &= (1-u)\,i_1 - ui_2 \\
L_2 \frac{di_2}{dt} &= u\upsilon_1 - \upsilon_2 + uE \\
C_2 \frac{d\upsilon_2}{dt} &= i_2 - \frac{\upsilon_2}{R}
\end{aligned} \tag{2.62}
$$

2.8.2 Normalization

After the required change of state and time variables one obtains the following normalized model for the converter:

$$
\begin{aligned}
\dot{x}_1 &= -(1-u)\,x_2 + u \\
\dot{x}_2 &= (1-u)\,x_1 - ux_3 \\
\alpha_1 \dot{x}_3 &= ux_2 - x_4 + u \\
\alpha_2 \dot{x}_4 &= x_3 - \frac{x_4}{Q}
\end{aligned} \tag{2.63}
$$

with

$$
\alpha_1 = L_2/L_1, \qquad \alpha_2 = C_2/C_1, \qquad Q = R\sqrt{C_1/L_1} \tag{2.64}
$$

2.8.3 Equilibrium Point and Static Transfer Function

The equilibrium equations are given by

$$
\begin{pmatrix} 0 & -(1-U) & 0 & 0 \\ 1-U & 0 & -U & 0 \\ 0 & U & 0 & -1 \\ 0 & 0 & 1 & -\frac{1}{Q} \end{pmatrix} \begin{pmatrix} \overline{x}_1 \\ \overline{x}_2 \\ \overline{x}_3 \\ \overline{x}_4 \end{pmatrix} = \begin{pmatrix} -U \\ 0 \\ -U \\ 0 \end{pmatrix} \tag{2.65}
$$

The average normalized equilibrium point, parameterized in terms of $u_{av} = U$ is found to be given by

$$
\overline{x}_1 = \frac{1}{Q}\frac{U^2}{(1-U)^2}, \qquad \overline{x}_2 = \frac{U}{1-U}, \qquad \overline{x}_3 = \frac{1}{Q}\frac{U}{(1-U)}, \qquad \overline{x}_4 = \frac{U}{1-U} \tag{2.66}
$$

A parametrization in terms of the desired output equilibrium voltage $\overline{x}_4$ is found by elimination of the parameter U, yielding:

$$
\overline{x}_1 = \frac{\overline{x}_4^2}{Q}, \qquad \overline{x}_2 = \overline{x}_4, \qquad \overline{x}_3 = \frac{\overline{x}_4}{Q}, \qquad U = \frac{\overline{x}_4}{\overline{x}_4 + 1} \tag{2.67}
$$

The static transfer function is hence given by:

$$\mathcal{H}(U) = \overline{x}_4 = \frac{U}{(1-U)} \tag{2.68}$$

which confirms the basic features of the Zeta converter as a possible *scaling* or *amplifying* converter.

The characteristic curve of the static transfer function is shown in Figure 2.35.

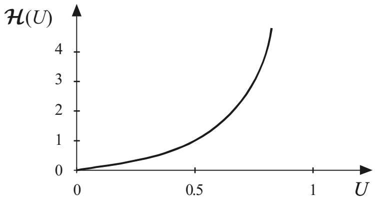

Fig. 2.35. Characteristic curve of the static transfer function for the Zeta DC-to-DC power converter.

2.9 The Quadratic Buck Converter

The quadratic Buck converter owes its name to the quadratic nature of the static transfer function in terms of a constant average control input value. This quadratic feature enhances the adjustment properties of the steady state equilibrium when the input is found to be close to the saturation limits. Here, we summarize the modelling features of a quadratic Buck converter shown in Figure 2.36.

2.9.1 Model of the Converter

$$\begin{aligned}
L_1 \frac{di_1}{dt} &= -v_1 + uE \\
C_1 \frac{dv_1}{dt} &= i_1 - ui_2 \\
L_2 \frac{di_2}{dt} &= uv_1 - v_2 \\
C_2 \frac{dv_2}{dt} &= i_2 - \frac{v_2}{R}
\end{aligned} \tag{2.69}$$

Circuit Diagram

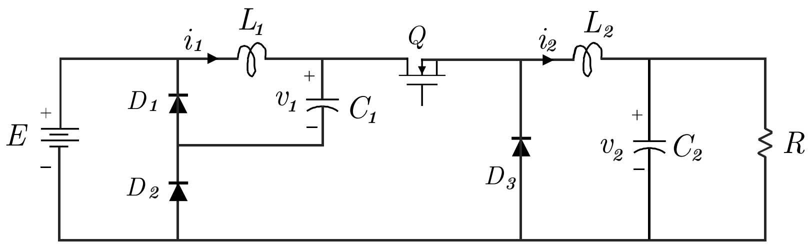

Fig. 2.36. The quadratic Buck converter with semiconductor realizations of the switches.

Ideal Circuit Realization

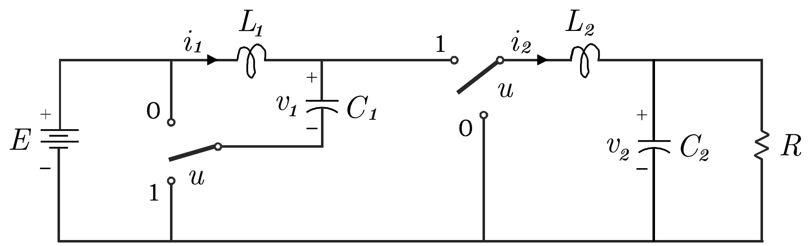

Fig. 2.37. Ideal switches realization of the quadratic Buck converter.

2.9.2 Normalized Model

$$\begin{aligned} \dot{x}_1 &= -x_2 + u \\ \dot{x}_2 &= x_1 - ux_3 \\ \alpha_1\dot{x}_3 &= ux_2 - x_4 \\ \alpha_2\dot{x}_4 &= x_3 - \frac{x_4}{Q} \end{aligned} \tag{2.70}$$

with,

$$\alpha_1 = L_2/L_1, \qquad \alpha_2 = C_2/C_1, \qquad Q = R\sqrt{C_1/L_1} \tag{2.71}$$

2.9.3 Equilibrium Point

The equilibrium points, parameterized in terms of a constant value U of the average control input, are found to be:

$$\overline{x}_1 = \frac{1}{Q}U^3, \qquad \overline{x}_2 = U, \qquad \overline{x}_3 = \frac{1}{Q}U^2, \qquad \overline{x}_4 = U^2 \tag{2.72}$$

These equilibrium points, parameterized now in terms of constant output voltage $\overline{x}_4$, are written as:

$$\overline{x}_1 = \frac{1}{Q}\left(\overline{x}_4\right)^{3/2}, \qquad \overline{x}_2 = \left(\overline{x}_4\right)^{1/2}, \qquad \overline{x}_3 = \frac{1}{Q}\overline{x}_4 \tag{2.73}$$

2.9.4 Static Transfer Function

The static transfer function of the quadratic Buck converter is obtained from (2.72) as:

$$\mathcal{H}\left(U\right) = \overline{x}_4 = U^2 \tag{2.74}$$

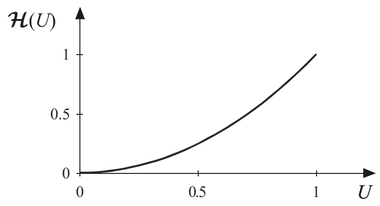

Fig. 2.38. Characteristic curve of the static transfer function for the quadratic Buck DC-to-DC power converter.

2.10 The Boost-Boost Converter

A tandem connection of two Boost converters, while preserving the independence of the control switches, results in a multi-variable DC-to-DC power converter. This converter has interest in applications where two loads need to be independently controlled with a single converter device. With some limitations, this is possible using the described combination of Boost converters.

Figure 2.39 depicts the Boost-Boost circuit with the switches realized by suitable arrangement of diodes and transistors.

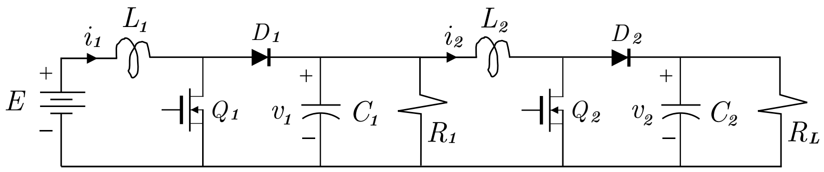

Fig. 2.39. The Boost-Boost circuit.

A realization of the circuit, entitling ideal switches, is shown in Figure 2.40.

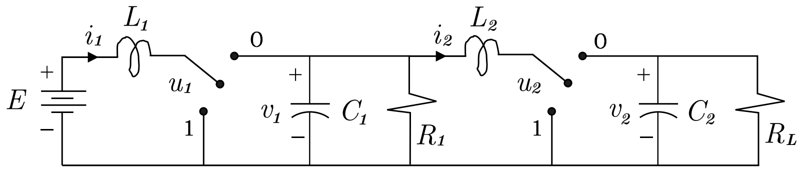

Fig. 2.40. Ideal switch realization of the Boost-Boost converter.

2.10.1 Model of the Boost-Boost Converter

$$\begin{aligned}
L_1 \frac{di_1}{dt} &= -\left(1-u_1\right) v_1 + E \\
C_1 \frac{dv_1}{dt} &= \left(1-u_1\right) i_1 - \frac{v_1}{R_1} - i_2 \\
L_2 \frac{di_2}{dt} &= v_1 - \left(1-u_2\right) v_2 \\
C_2 \frac{dv_2}{dt} &= \left(1-u_2\right) i_2 - \frac{v_2}{R_L}
\end{aligned} \tag{2.75}$$

2.10.2 Average Normalized Model

$$\begin{aligned}
\frac{dx_1}{d\tau} &= -\left(1-u_{1av}\right) x_2 + 1 \\
\frac{dx_2}{d\tau} &= \left(1-u_{1av}\right) x_1 - \frac{1}{Q_1} x_2 - x_3 \\
\alpha_1 \frac{dx_3}{d\tau} &= x_2 - \left(1-u_{2av}\right) x_4 \\
\alpha_2 \frac{dx_4}{d\tau} &= \left(1-u_{2av}\right) x_3 - \frac{1}{Q_L} x_4
\end{aligned} \tag{2.76}$$

with,

$$\alpha_1 = \frac{L_2}{L_1}, \qquad \alpha_2 = \frac{C_2}{C_1}, \qquad Q_1 = R_1 \sqrt{\frac{C_1}{L_1}}, \qquad Q_L = R_L \sqrt{\frac{C_1}{L_1}} \tag{2.77}$$

2.10.3 Equilibrium Point and Static Transfer Function

Under the assumption of constant average control inputs U_1 and U_2 we find the following equations for the state equilibrium point,

$$\begin{pmatrix} 0 & -(1-U_1) & 0 & 0 \\ (1-U_1) & -\frac{1}{Q_1} & -1 & 0 \\ 0 & 1 & 0 & -(1-U_2) \\ 0 & 0 & (1-U_2) & -\frac{1}{Q_L} \end{pmatrix} \begin{pmatrix} \overline{x}_1 \\ \overline{x}_2 \\ \overline{x}_3 \\ \overline{x}_4 \end{pmatrix} = \begin{pmatrix} -1 \\ 0 \\ 0 \\ 0 \end{pmatrix} \tag{2.78}$$

The solution of the above equations, parameterized by the constant values of the average control inputs is given by

$$\begin{pmatrix} \overline{x}_1 \\ \overline{x}_2 \\ \overline{x}_3 \\ \overline{x}_4 \end{pmatrix} = \begin{pmatrix} \frac{1}{Q_1 Q_L} \frac{Q_1 + Q_L (1-U_2)^2}{(1-U_1)^2 (1-U_2)^2} \\ \frac{1}{1-U_1} \\ \frac{1}{Q_L} \frac{1}{(1-U_1)(1-U_2)^2} \\ \frac{1}{(1-U_1)(1-U_2)} \end{pmatrix} \tag{2.79}$$

The output variables of the Boost-Boost converter are considered to be the voltage variables, x_2 and x_4. A parametrization of the equilibrium point in terms of the steady state output voltages: $\overline{x}_2 = V_{2d}$ and $\overline{x}_4 = V_{4d}$, is obtained as

$$\overline{x}_1 = \frac{V_{2d}^2}{Q_1} + \frac{V_{4d}^2}{Q_L}, \qquad \overline{x}_2 = V_{2d}, \qquad \overline{x}_3 = \frac{V_{4d}^2}{Q_L V_{2d}}, \qquad \overline{x}_4 = V_{4d} \tag{2.80}$$

where:

$$U_1 = \frac{V_{2d} - 1}{V_{2d}}, \qquad U_2 = \frac{V_{4d} - V_{2d}}{V_{4d}} \tag{2.81}$$

Such an equilibrium point, in original state variables, is found to be:

$$\bar{i}_1 = \frac{1}{R_1} \frac{\overline{v}_1^2}{E} + \frac{1}{R_L} \frac{\overline{v}_2^2}{E}, \qquad \bar{i}_2 = \frac{1}{R_L} \frac{\overline{v}_2^2}{\overline{v}_1} \tag{2.82}$$

and

$$\overline{v}_1 = \frac{1}{(1-U_1)} E, \qquad \overline{v}_2 = \frac{1}{(1-U_1)(1-U_2)} E \tag{2.83}$$

Therefore

$$U_1 = 1 - \frac{E}{\overline{v}_1}, \qquad U_2 = 1 - \frac{\overline{v}_1}{\overline{v}_2} \tag{2.84}$$

The *normalized static transfer matrix* is now defined as a *row vector* relating the two output voltages with the scalar constant input voltage. Evidently, the entries of such a matrix are now functions of U_1 and U_2. This matrix is constituted by the steady state values of the output voltages. We have

$$\mathcal{H}(U_1, U_2) = \left[\overline{x}_2(U_1, U_2) \; \overline{x}_4(U_1, U_2) \right] = \left[\frac{1}{1-U_1} \;\; \frac{1}{(1-U_1)(1-U_2)} \right] \tag{2.85}$$

2.10.4 Alternative Model of the Boost-Boost Converter

In order to simplify the manipulations involved in the controller design for the multi-variable Boost-Boost converter, we present the alternative average model of the system in the same spirit as that presented for the mono-variable case.

$$\begin{aligned}
\frac{dx_1}{d\tau} &= -\mathbf{u}_{1av}x_2 + 1 \\
\frac{dx_2}{d\tau} &= \mathbf{u}_{1av}x_1 - \frac{1}{Q_1}x_2 - x_3 \\
\alpha_1\frac{dx_3}{d\tau} &= x_2 - \mathbf{u}_{2av}x_4 \\
\alpha_2\frac{dx_4}{d\tau} &= \mathbf{u}_{2av}x_3 - \frac{1}{Q_L}x_4
\end{aligned} \tag{2.86}$$

Clearly, we have defined the following new control inputs:

$$\mathbf{u}_{1av} = (1 - u_{1av}) \tag{2.87}$$

$$\mathbf{u}_{2av} = (1 - u_{2av}) \tag{2.88}$$

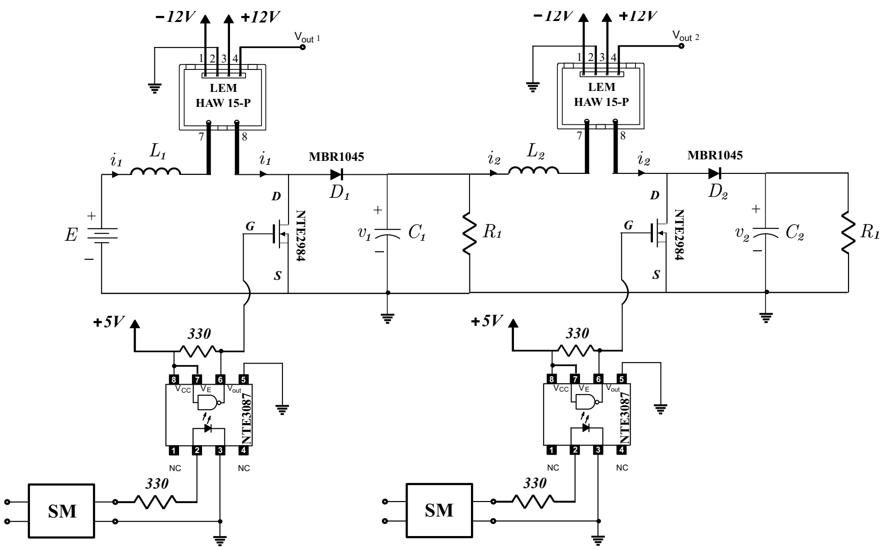

Fig. 2.41. Circuit diagram of the *Boost-Boost converter prototype.*

2.10.5 A Boost-Boost Converter Experimental Prototype

The actual circuit and a picture of the *Boost-Boost system* are shown in Figures 2.41, and 2.42, respectively. We have set the following parameter values:

$$L_1 = 15.91 \text{ mH}, \qquad C_1 = 48 \ \mu\text{F}, \qquad L_2 = 40 \text{ mH}, \qquad C_2 = 107 \ \mu\text{F},$$

$$R_1 = 52 \ \Omega, \qquad R_L = 52 \ \Omega, \qquad E = 12 \text{ V}$$

The switching frequency for the Boost-Boost converter, as in the previous converters, is 45 kHz. Thus, the inductors L_1 and L_2 were designed for this operation frequency.

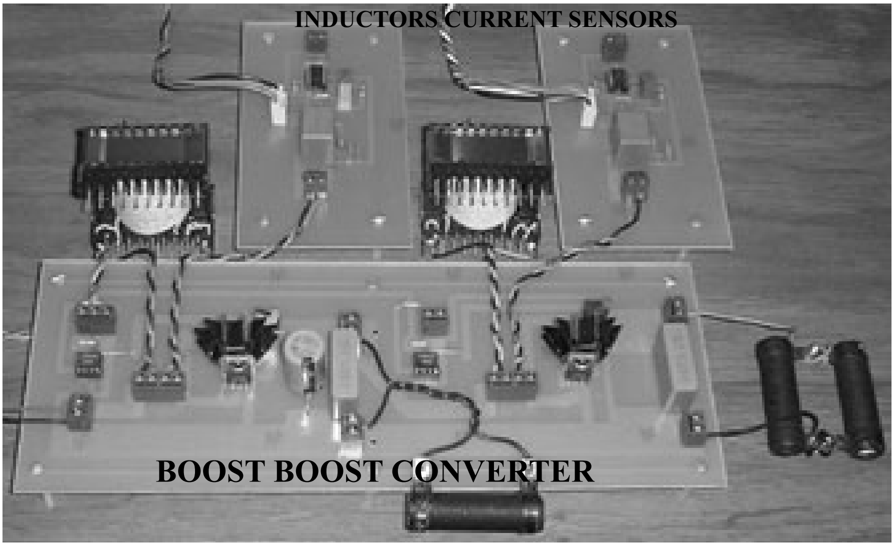

Fig. 2.42. Photograph of the *Boost-Boost system.*

2.11 The Double Buck-Boost Converter

Similarly to the Boost-Boost system, we propose a double Buck-Boost converter as a multi-variable DC-to-DC power converter with interesting, but limited, independence features for handling two loads with different steady state, or tracking, requirements. As in the previous case we limit ourselves to a summary of the relevant equations of the model and the steady state features.

Figure 2.43 depicts the tandem connection of two Buck-Boost DC-to-DC power converters.

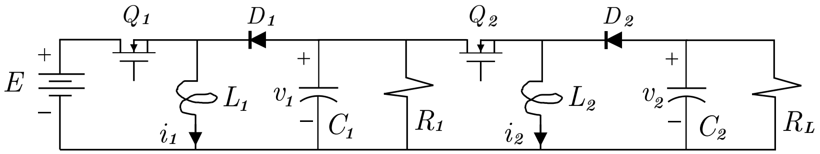

Fig. 2.43. Double Buck-Boost converter circuit.

2.11.1 Model of the Double Buck-Boost Converter

$$
\begin{aligned}
L_1 \frac{di_1}{dt} &= (1-u_1)\,\upsilon_1 + u_1 E \\
C_1 \frac{d\upsilon_1}{dt} &= -(1-u_1)\,i_1 - \frac{\upsilon_1}{R_1} - u_2 i_2 \\
L_2 \frac{di_2}{dt} &= u_2 \upsilon_1 + (1-u_2)\,\upsilon_2 \\
C_2 \frac{d\upsilon_2}{dt} &= -(1-u_2)\,i_2 - \frac{\upsilon_2}{R_L}
\end{aligned}
\tag{2.89}
$$

2.11.2 Average Normalized Model

$$
\begin{aligned}
\frac{dx_1}{d\tau} &= (1-u_{1av})\,x_2 + u_{1av} \\
\frac{dx_2}{d\tau} &= -(1-u_{1av})\,x_1 - \frac{1}{Q_1}x_2 - u_{2av}x_3 \\
\alpha_1 \frac{dx_3}{d\tau} &= u_{2av}x_2 + (1-u_{2av})\,x_4 \\
\alpha_2 \frac{dx_4}{d\tau} &= -(1-u_{2av})\,x_3 - \frac{1}{Q_L}x_4
\end{aligned}
\tag{2.90}
$$

with,

$$
\alpha_1 = \frac{L_2}{L_1}, \qquad \alpha_2 = \frac{C_2}{C_1}, \qquad Q_1 = R_1\sqrt{\frac{C_1}{L_1}}, \qquad Q_L = R_L\sqrt{\frac{C_1}{L_1}} \tag{2.91}
$$

2.11.3 Equilibrium Point and Static Transfer Function

The parametrization of the equilibrium point in terms of U_1 and U_2 is found to be

$$
\begin{pmatrix} \overline{x}_1 \\ \overline{x}_2 \\ \overline{x}_3 \\ \overline{x}_4 \end{pmatrix} = \begin{pmatrix} \frac{U_1}{Q_1 Q_L}\frac{Q_1 U_2^2 + Q_L(1-U_2)^2 +}{(1-U_1)^2(1-U_2)^2} \\ -\frac{U_1}{1-U_1} \\ -\frac{1}{Q_L}\frac{U_1 U_2}{(1-U_1)(1-U_2)^2} \\ \frac{U_1 U_2}{(1-U_1)(1-U_2)} \end{pmatrix} \tag{2.92}
$$

The parametrization in terms of the desired output voltages $\overline{x}_2 = V_{2d}$ and $\overline{x}_4 = V_{4d}$, is found to be

$$\overline{x}_1 = -\left(\frac{V_{2d}^2}{Q_1} + \frac{V_{4d}^2}{Q_L}\right)\left(\frac{1 - V_{2d}}{V_{2d}}\right), \; \overline{x}_2 = V_{2d}, \; \overline{x}_3 = \frac{V_{4d}}{Q_L}\left(\frac{V_{4d}}{V_{2d}} - 1\right), \; \overline{x}_4 = V_{4d} \tag{2.93}$$

where

$$U_1 = -\frac{V_{2d}}{1 - V_{2d}}, \qquad U_2 = \frac{V_{4d}}{V_{4d} - V_{2d}} \tag{2.94}$$

The normalized static transfer matrix is, as before, given by a row vector whose entries are functions of U_1 and U_2,

$$\mathcal{H}(U_1, U_2) = \left[-\frac{U_1}{1-U_1} \;\; \frac{U_1 U_2}{(1-U_1)(1-U_2)} \right] \tag{2.95}$$

2.12 Power Converter Models with Non-ideal Components

In this chapter, we have emphasized ideal components in the constitution of dynamical average DC-to-DC power converter models. For instance, we have not considered resistances in series with the inductors, we have neglected parallel conductances in combination with capacitors and have also assumed that the switches have no imperfections attached. In real life, inductors do exhibit associated resistances, capacitors must be considered along with parallel conductances, or equivalent series resistances, and switches are synthesized by means of physical transistor and diode arrangements which exhibit important resistances and parasitic voltage sources.

A more realistic model of a DC-to-DC power converter must, therefore, include a number of "parasitic" resistances and voltage sources in connection with the diode-transistor arrangements synthesizing the regulating switch. Here we will only present one such example, concerning the "Boost" converter model, in order to highlight the important differences with the already derived ideal model.

Figure 2.44 shows a Boost converter model including parasitic components surrounding the ideal switch. The model of such a converter, using the Kirchoff's voltage and current laws as in the several previous examples presented in this chapter, results in the following set of differential equations (see also Ortega *et al.* [48])

$$\begin{aligned}
\dot{x}_1 &= -\frac{r}{L}x_1 - u\frac{R}{(r_C + R)L}x_2 + \frac{E}{L} - u\frac{V_F}{L} \\
\dot{x}_2 &= u\frac{R}{(r_C + R)C}x_1 - \frac{1}{(r_C + R)C}x_2 \\
x_0 &= \frac{R}{r_C + R}x_2 + u\frac{r_C R}{r_C + R}x_1
\end{aligned}$$

where $(r_C||R)$ stands for the resistance associated with the parallel arrangement of resistors of values: r_C and R. The resistance r is given by

$$r = [r_L + (1-u)r_{DS} + u\,(R_F + (r_C||R))]$$

The variable x_0 is the output voltage which, in this instance, is not directly constituted by the capacitor voltage x_2 and directly receives the influence of x_1 and of the control input variable u. Note that if the values of the parasitic resistances described by r_C, r_L and r_{DS} are all set to zero, we recover the ideal model of the "Boost" converter.

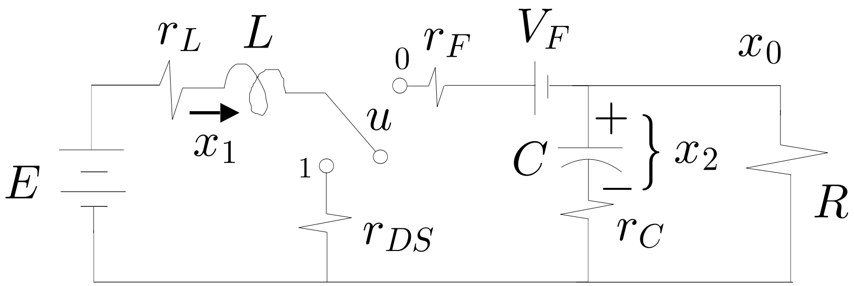

Fig. 2.44. A realistic model of the Boost converter.

A rigorous mathematical analysis aimed at the derivation of control laws for a DC-to-DC power converter should entitle a realistic model of the converter of the same nature as that described in the previous paragraphs for the Boost converter. However, experience tells that the complexity of the derivations associated with such models does not substantially improve the quality of the overall converter performance, as far as the closed loop operation is concerned, when compared with that achieved by a controller derived in terms of the idealized models. Naturally, the fundamental discrepancies refer to *constant* steady state stabilization or tracking errors, and transients quality. These features may, in principle, be remedied by automatic adjustment features (say, of the integral tracking error type) bestowed on the simplified controller. Nevertheless, in order to justify the assertion we have just made, we state that *all* the laboratory tests of controller performance, carried out on the actual prototypes described in this book, involved controller designs entirely based on the ideal models.

2.13 A General Mathematical Model for Power Electronics Devices

Most of power electronics devices, such as: DC-to-DC power converters, DC-to-AC converters, ac rectifiers, inverters, and combinations of these devices with dc and ac electric motors are accurately described by nonlinear system models of varying complexity. A closer examination of such models reveals that even though these systems are nonlinear, they belong, generally speaking, to the class of *bilinear* systems. As such, it is also revealing to study the "energy dissipation structure" of most of these dynamic models.

In a state space framework viewpoint electric circuits are considered as *lumped parameter* dynamical systems. this is the case of electric and electronic circuits in general, as opposed to *distributed* i.e., infinite dimensional circuits. Lumped parameter circuits are described, in general, by ordinary nonlinear vector differential equations. The right hand side of these systems of equations are vectors which depend nonlinearly on the state vector of the system, These nonlinear vector functions are generally addressed as *vector fields.* The presence of control inputs in the right hand side of the describing differential equations is termed *controlled vector fields.* A nonlinear dynamic system is then generally described by the set of equations

$$\dot{x} = f(x, u) \tag{2.96}$$

where x is a vector in R^n and the control input $u \in R^m$. The nonlinear map f is assumed to be either *smooth*, i.e., it admits an infinite number of derivatives with respect to its arguments, of *analytic* i.e., at any point in the (x, u) space we can obtain a infinite convergent Taylor series expansion of the function $f(x, u)$. In the description of power electronics devices, the control input functions u represent, in general, *switch position functions*, i.e., each component of the vector u independently takes values in a *discrete set.* In some instances such set is represented by a binary set with two numerical values, say $\{0, 1\}$. In other instances, such binary set is of the form $\{-W, +W\}$ where W is a constant real number. We denote the set where the switched control input vector takes values by a "power" of the binary set where each component takes values: i.e., $\{0, 1\}^m$, or $\{-W, W\}^m$. Such powers evidently mean, cartesian products of the base set a finite number of times defined by m.

Power electronics models are thus, generally speaking, *Variable Structure Systems.* This class of systems is naturally characterized by the possibility of sudden changes in their differential equation description. This immediately translates, in the circuit description arena, to a sudden change in the *circuit topology.* Such topological changes may be made 1) "occasionally" in a non-periodic fashion, 2) periodically, with a significant frequency or, even, at an ideally *infinite* frequency rate. This last idealization, most often, proves to be useful in rescuing the main qualitative features of high-frequency topological changes (such as those provided, say, by a PWM train of pulses triggering such topology changes), without resorting to exact or approximate discretizations of the nonlinear set of differential equations describing the power device. In general, we term such ideally infinite frequency models as *average* models. These average models are most suitable for feedback control considerations. With an abuse of notation, we customarily mathematically describe such average models with the same symbols for state variables as in the switched model, except for a distinction in the control input. We write,

$$\dot{x} = f(x, u_{av}) \tag{2.97}$$

where now x is addressed as the average state vector, still taking values in R^n and u_{av} is now a *continuous* valued m-dimensional function. The average control input functions u_{av} are now *bounded* functions continuously taking values over compact sets in R^m. If the original control input function components $u_i, i = 1, ..., m$ take values, independently, on, say, the binary set $\{0, 1\}$, then the components of the average control input vector u_{av} will take values on the closed interval $[0, 1]$ of the real line. Hence, the vector u_{av} takes values on $[0, 1]^m$.

The most general model one can think of, for power electronics devices, clearly exhibits the following decomposition of the "energy managing" structure: 1) An input dependent conservative vector field, characterized by the product of a skew symmetric matrix with the state vector. The skew symmetric matrix is, generally speaking, an affine function of the input vector components and its most important property is that it does not intervene in the system stability considerations. 2) A dissipative vector field characterized by the product of a constant symmetric, positive semi-definite, matrix with the state vector. This term accounts for the dissipation forces in the system due to resistances and frictions. 3) The control input channels which entitle a constant matrix multiplying the input vector. The input vector is constituted by switching functions representing the discontinuous control inputs to the system. 4) A time varying or, alternatively constant, vector field representing the external input sources. Such sources are of fixed nature, i.e., their amplitude values and frequencies are not subject to our command. The sum of this various fields produces the rate of change of the state of the system. Such a general model is summarized in the following n-dimensional differential equation:

$$\mathcal{A}\dot{x} = \mathcal{J}(u)x - \mathcal{R}x + \mathcal{B}u + \mathcal{E}(t) \tag{2.98}$$

where: x is an n-dimensional vector, $\mathcal{A}$ is a symmetric, positive definite, constant, matrix, $\mathcal{J}$ is a skew symmetric matrix of the form:

$$\mathcal{J} = \mathcal{J}_0 + \sum_{i=1}^{m} \mathcal{J}_i u_{i\ av} \tag{2.99}$$

for all u_i, where $\mathcal{J}_0$ is constant and skew symmetric and $\mathcal{J}_i$ is also constant skew symmetric for all i. $\mathcal{R}$ is a symmetric, positive semi-definite constant matrix. $\mathcal{B}$ is a constant $n \times m$ matrix and, hence y is an m dimensional output vector. In terms of its n dimensional column vectors, the matrix $\mathcal{B}$ is given by $\mathcal{B} = [b_1, b_2, \cdots, b_m]$. The vector u_{av} is the average control input vector assumed to be m-dimensional, with each component $u_{i\,av}$ taking values either in the closed set $[0, 1]$, or in the closed set $[-1, 1]$, of the real line. In any case, $u_{i\,av}$ represents a *bounded* average control input function. $\mathcal{E}(t)$ is a n-dimensional smooth vector function of t or, sometimes, a vector of constant entries.

Note that the matrix $\mathcal{R}$ represents the *dissipative field* of the system while $\mathcal{J}(u)$ represents the, possibly control input dependent, *conservative field* of the system. The *control input channels* are represented by the constant matrix $\mathcal{B}$ while $\mathcal{E}(t)$ represent *external input sources*, such as batteries or ac line voltages.

We will be using this rather general *bilinear system* model, rather extensively, in later chapters in connection with linear feedback controller designs for power electronics devices. The average models, or infinite frequency models, corresponding to this general mathematical model will be described by the following set of controlled differential equations:

$$\mathcal{A}\dot{x} = \mathcal{J}(u_{av})x - \mathcal{R}x + \mathcal{B}u_{av} + \mathcal{E}(t) \tag{2.100}$$

The general model (2.100) has a number of interesting properties which enormously ease the feedback controller design task. We defer the study of the mathematical properties of this model to Chapter 5, where we address the study of nonlinear methods for controller design.

2.13.1 Some Illustrative Examples of the General Model

Here, we present just a couple of examples illustrating the validity of the general mathematical model, proposed in this section, in relation to some DC-to-DC power converter models. In Chapter 7 we shall also use this general model for monophasic and three phase rectifiers. The general model is also valid for power converters loaded by DC motors as well as mono and three -phase rectifiers loaded with DC motors.

The Boost-Boost Converter

Consider the following average normalized model of the Boost-Boost converter.

$$\begin{aligned}
\frac{dx_1}{d\tau} &= -u_{1av}x_2 + 1, \qquad & \frac{dx_2}{d\tau} &= u_{1av}x_1 - \frac{1}{Q_1}x_2 - x_3 \\
\alpha_1\frac{dx_3}{d\tau} &= x_2 - u_{2av}x_4, \qquad & \alpha_2\frac{dx_4}{d\tau} &= u_{2av}x_3 - \frac{1}{Q_L}x_4
\end{aligned} \tag{2.101}$$

The mathematical model of the average normalized Boost-Boost converter may be written, in matrix form, as:

$$\begin{bmatrix} 1 & 0 & 0 & 0 \\ 0 & 1 & 0 & 0 \\ 0 & 0 & \alpha_1 & 0 \\ 0 & 0 & 0 & \alpha_2 \end{bmatrix} \begin{bmatrix} \dot{x}_1 \\ \dot{x}_2 \\ \dot{x}_3 \\ \dot{x}_4 \end{bmatrix} = \begin{bmatrix} 0 & -u_{1av} & 0 & 0 \\ u_{1av} & 0 & -1 & 0 \\ 0 & 1 & 0 & -u_{2av} \\ 0 & 0 & u_{2av} & 0 \end{bmatrix} \begin{bmatrix} x_1 \\ x_2 \\ x_3 \\ x_4 \end{bmatrix} - \begin{bmatrix} 0 & 0 & 0 & 0 \\ 0 & \frac{1}{Q_1} & 0 & 0 \\ 0 & 0 & 0 & 0 \\ 0 & 0 & 0 & \frac{1}{Q_L} \end{bmatrix} \begin{bmatrix} x_1 \\ x_2 \\ x_3 \\ x_4 \end{bmatrix} + \begin{bmatrix} 1 \\ 0 \\ 0 \\ 0 \end{bmatrix}$$

Hence, in reference to the proposed general model (2.100) we have

$$\mathcal{A} = \begin{bmatrix} 1 & 0 & 0 & 0 \\ 0 & 1 & 0 & 0 \\ 0 & 0 & \alpha_1 & 0 \\ 0 & 0 & 0 & \alpha_2 \end{bmatrix}, \quad \mathcal{R} = \begin{bmatrix} 0 & 0 & 0 & 0 \\ 0 & \frac{1}{Q_1} & 0 & 0 \\ 0 & 0 & 0 & 0 \\ 0 & 0 & 0 & \frac{1}{Q_L} \end{bmatrix}, \quad \mathcal{B} = b = 0, \quad \mathcal{E} = \begin{bmatrix} 1 \\ 0 \\ 0 \\ 0 \end{bmatrix}$$

$$\begin{aligned} \mathcal{J}(u_{av}) &= \mathcal{J}_0 + \mathcal{J}_1 u_{1av} + \mathcal{J}_2 u_{2av} \\ &= \begin{bmatrix} 0 & 0 & 0 & 0 \\ 0 & 0 & -1 & 0 \\ 0 & 1 & 0 & 0 \\ 0 & 0 & 0 & 0 \end{bmatrix} + \begin{bmatrix} 0 & -1 & 0 & 0 \\ 1 & 0 & 0 & 0 \\ 0 & 0 & 0 & 0 \\ 0 & 0 & 0 & 0 \end{bmatrix} u_{1av} + \begin{bmatrix} 0 & 0 & 0 & 0 \\ 0 & 0 & 0 & 0 \\ 0 & 0 & 0 & -1 \\ 0 & 0 & 1 & 0 \end{bmatrix} u_{2av} \end{aligned}$$

The Sepic Converter

Consider now, the following average normalized model of the Sepic converter:

$$\begin{aligned} \dot{x}_1 &= -(1 - u_{av})(x_2 + x_4) + 1 \\ \dot{x}_2 &= (1 - u_{av}) x_1 - u_{av} x_3 \\ \alpha_1 \dot{x}_3 &= u_{av} x_2 - (1 - u_{av}) x_4 \\ \alpha_2 \dot{x}_4 &= (1 - u_{av})(x_1 + x_3) - \frac{x_4}{Q} \end{aligned} \tag{2.102}$$

Writing the model in matrix form we have:

$$\begin{bmatrix} 1 & 0 & 0 & 0 \\ 0 & 1 & 0 & 0 \\ 0 & 0 & \alpha_1 & 0 \\ 0 & 0 & 0 & \alpha_2 \end{bmatrix} \begin{bmatrix} \dot{x}_1 \\ \dot{x}_2 \\ \dot{x}_3 \\ \dot{x}_4 \end{bmatrix} = \begin{bmatrix} 0 & -(1-u_{av}) & 0 & -(1-u_{av}) \\ 1-u_{av} & 0 & -u_{av} & 0 \\ 0 & u_{av} & 0 & -(1-u_{av}) \\ 1-u_{av} & 0 & 1-u_{av} & 0 \end{bmatrix} \begin{bmatrix} x_1 \\ x_2 \\ x_3 \\ x_4 \end{bmatrix} - \begin{bmatrix} 0 & 0 & 0 & 0 \\ 0 & 0 & 0 & 0 \\ 0 & 0 & 0 & 0 \\ 0 & 0 & 0 & \frac{1}{Q} \end{bmatrix} \begin{bmatrix} x_1 \\ x_2 \\ x_3 \\ x_4 \end{bmatrix} + \begin{bmatrix} 1 \\ 0 \\ 0 \\ 0 \end{bmatrix}$$

In reference to the proposed general model (2.100), we have:

$$\mathcal{A} = \begin{bmatrix} 1 & 0 & 0 & 0 \\ 0 & 1 & 0 & 0 \\ 0 & 0 & \alpha_1 & 0 \\ 0 & 0 & 0 & \alpha_2 \end{bmatrix}, \quad \mathcal{R} = \begin{bmatrix} 0 & 0 & 0 & 0 \\ 0 & 0 & 0 & 0 \\ 0 & 0 & 0 & 0 \\ 0 & 0 & 0 & \frac{1}{Q} \end{bmatrix}, \quad \mathcal{B} = b = 0, \quad \mathcal{E} = \begin{bmatrix} 1 \\ 0 \\ 0 \\ 0 \end{bmatrix}$$

$$\mathcal{J}(u_{av}) = \mathcal{J}_0 + \mathcal{J}_1 u_{av} = \begin{bmatrix} 0 & -1 & 0 & -1 \\ 1 & 0 & 0 & 0 \\ 0 & 0 & 0 & -1 \\ 1 & 0 & 1 & 0 \end{bmatrix} + \begin{bmatrix} 0 & 1 & 0 & 1 \\ -1 & 0 & -1 & 0 \\ 0 & 1 & 0 & 1 \\ -1 & 0 & -1 & 0 \end{bmatrix} u_{av}$$

The proposed mathematical model is also valid for original (i.e., non-normalized) switched DC-to-DC power converter models when they are suitably rewritten in matrix form. We leave it to the reader to verify that anyone of the converter models presented in this chapter, except for the Boost converter exhibiting realistic parasitic components, conform to the general mathematical model (2.100).

When parasitic components are considered, the symmetric dissipative matrix $\mathcal{R}$ may be an affine function of the control input, i.e., we must consider control dependent dissipations, $\mathcal{R}(u) = \mathcal{R}_0 + \mathcal{R}_1 u$.

http://www.springer.com/978-1-84628-458-8

Control Design Techniques in Power Electronics Devices
Sira-Ramirez, H.; Silva-Ortigoza, R.
2006, XVII, 423 p., Hardcover
ISBN: 978-1-84628-458-8